THE INVESTIGATION OF THE DYNAMIC COMPRESSION CHARACTERISTICS OF A LAYERED GLASS SYSTEM

A Thesis Submitted to
the Graduate School of
İzmir Institute of Technology
in Partial Fulfillment of the Requirements for the Degree of

MASTER OF SCIENCE

in Mechanical Engineering

by
Burak AĞIRDICI

July 2023
İZMİR

We approve the thesis of **Burak AĞIRDICI**

Examining Committee Members:

Prof. Dr. Alper TAŞDEMİRCİ
Department of Mechanical Engineering, İzmir Institute of Technology

Prof. Dr. Hatice Seçil ARTEM
Department of Mechanical Engineering, İzmir Institute of Technology

Prof. Dr. Evren Meltem TOYGAR
Department of Mechanical Engineering, Dokuz Eylül University

5 July 2023

Prof. Dr. Alper TAŞDEMİRCİ
Supervisor, Department of
Mechanical Engineering
İzmir Institute of Technology

Prof. Dr. M. İ. Can DEDE
Head of the Department of
Mechanical Engineering

Prof. Dr. Mehtap EANES
Dean of the Graduate School of
Engineering and Sciences

ACKNOWLEDGMENTS

First, I would like to express my gratitude and respect to my esteemed advisor, Prof. Dr. Alper TAŞDEMİRCİ, who has made an important contribution to my professional development and whose moral support I have always felt during my master's degree.

I would like to thank my colleagues Mesut BAYHAN, Çetin BAKICI, Mustafa Kemal SARIKAYA, and Samed ENSER, who work in the Dynamic Testing and Modeling Laboratory, for sharing their knowledge and experience.

I would like to express my gratitude to my dear mother, Fatma AĞIRDICI, and my dear father, Fethi AĞIRDICI, who has never spared their moral and material contributions to raising me. I would like to express my special thanks to my brother Enis AĞIRDICI and his wife, Derya AĞIRDICI, who encouraged me to start my academic career.

I would like to thank my dear friends Eyüpcan EVKAN and Recep Kürşad PEYNİRCİ, whose support I have always felt.

Finally, I would like to thank my pet Era, whose love I always feel.

ABSTRACT

THE INVESTIGATION OF THE DYNAMIC COMPRESSION CHARACTERISTICS OF A LAYERED GLASS SYSTEM

Layered glass structures are one of the most common material types used in air, land, and sea vehicles. Since these structures are exposed to external impact loads, it is important to determine their dynamic mechanical behavior. In this study, dynamic compression characteristics of the layered glass system were investigated numerically using the LS-DYNA finite element program. The Johnson Holmquist Ceramics material model was used for the glass layer, the Ogden Rubber material model, which is used in material models with high elastic structural behavior was used for the polyvinyl butyral (PVB) interlayer, and the SAMP-1 material model was used for the polycarbonate interlayer. Numerical studies were carried out to investigate the stress wave propagation, the amount of energy released, and the deceleration rate of the penetration velocity. Split Hopkinson Pressure Bar setup was used to numerically load the layered glass systems at high strain rates for a reliably easy controlled wave generation. The layered glass structure consisting of two interlayer types with different thicknesses was loaded in the SHPB system, and the effect of the interlayer material type and thickness on the stress wave propagation was investigated. Then, the projectile impact test was modeled at different impact velocities for a square plate of PVB-layered glass structure. The thickness of the PVB interlayer was kept constant, while the thickness and location of the glass layer varied. From the results, the slowing rate of the projectile, the amount of erosion energy, and the energy balance were determined.

ÖZET

KATMANLI BİR CAM SİSTEMİNİN DİNAMİK BASMA KARAKTERİSTİKLERİNİN İNCELENMESİ

Katmanlı cam yapılar hava, kara ve deniz araçlarında en yaygın kullanılan malzeme türlerinden biridir. Bu yapılar dış darbe yüklerine maruz kaldıklarından, dinamik mekanik davranışlarının belirlenmesi önemlidir. Bu çalışmada, katmanlı cam sisteminin dinamik basma karakteristikleri sayısal olarak LS-DYNA sonlu elemanlar programında incelendi. Cam katmanı için Johnson Holmquist Ceramics malzeme modeli, polivinil bütiral (PVB) ara katmanı için yüksek elastik yapısal davranışa sahip malzeme modellerinde kullanılan Ogden Rubber malzeme modeli ve polikarbonat ara katman için SAMP-1 malzeme modeli kullanıldı. Sayısal çalışmalar gerilme dalgası yayılımı, açığa çıkan enerji miktarı ve penetrasyon hızının yavaşlama oranını araştırmak için yapıldı. Güvenilir ve kolay kontrollü bir dalga üretimi için sayısal olarak katmanlı cam sistemlerini yüksek gerilim hızlarında yüklemek için Bölünmüş Hopkinson Basınç Çubuğu kurulumu kullanıldı. Farklı kalınlıklara sahip iki ara katman tipinden oluşan katmanlı cam yapı SHPB sisteminde yüklenmiş ve ara katman malzeme tipi ve kalınlığının gerilme dalgası yayılımına etkisi incelendi. Daha sonra, PVB-katmanlı cam yapının kare bir levhası için farklı darbe hızlarında mermi çarpma testi modellendi. PVB ara katmanının kalınlığı sabit tutulurken, cam katmanın kalınlığı ve yeri değişti. Analiz sonuçlarından merminin yavaşlama hızı, aşındırma enerjisi miktarı ve enerji dengesi belirlendi.

TABLE OF CONTENTS

LIST OF FIGURES

Figure **Page**

Figure **Page**

Figure **Page**

LIST OF TABLES

Table **Page**

CHAPTER 1

INTRODUCTION

Laminated glass is produced from at least two glass plates by combining the polymer interlayer material under heat and pressure. Layered glass reduces the risk of injury by preventing the scattering of glass pieces when breakage occurs. Due to this feature, it is also called safety glass. Since laminated glass presents better resistance against penetration, they are widely used in the defense, aerospace, and automotive industries. Layered glasses are generally formed by the combination of PVB or polycarbonate interlayers. The function of the interlayer is to keep the broken pieces together once laminated glass fractures, reducing the chance of glass shard injuries. In Figure 1.1, structures using laminated glass are shown schematically.

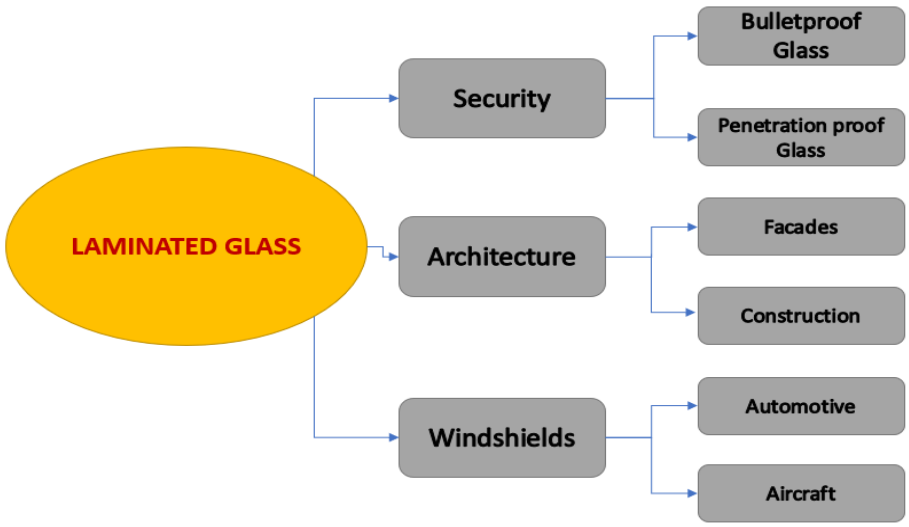

Figure 1.1 Applications of laminated glass

Layered glass is used for protection purposes in structures. Recently, the use of layered glass in architectural structures also has increased due to its better insulation characteristics against heat and sound. Layered glass structures have been used in air and land vehicles for many years. In Figure 1.2, examples of structures using laminated glass are given.

(a) (Source: wikipedia.com[1]) (b) (Source:guardianglass.com[2])

(c) (Source: swmintl.com[3]) (d) (Source: scienceabc.com[4])

Figure 1.2 Layered glass (a) Bulletproof, (b) Facades, (c) Aircraft, and (d) Automotive

A polymer interlayer is used very frequently in layered glass. The interlayer materials are Polyvinyl Butyral (PVB), Polycarbonate, Super Performance Grade (SPG) Polymer, Thermoplastic Polyurethane (TPU), etc. Mostly they present higher failure strain values.

1.1. Literature Review

It is important to perform analyzes of layered glass structures. Layered glass is often used in structures for safety reasons. Researchers continue to work to improve the mechanical behavior of the layered glass system. In this section, studies about layered glass in the literature were explained.

Dynamic compression and shear experiments of borosilicate glass material with a strain rate of approximately 250/s were performed by Nie et al.[5] using SHPB. A cubic

specimen of 12.5x8.9x8.9 mm was tested with angles of 0, 3, 5, and 7, respectively. Experimental data show that as the shear angle increased, the equivalent stress decreased and with the increase of the shear angle, cracks in the glass occur in certain regions.

Strassburger et al.[6] performed the Edge-on Impact tests at the soda-lime glass. Experimental and numerical results were compared. Grujicic et al.[7] referenced work by Strassburger. Solid steel projectiles in the shape of cylinders with radius of 15 mm and 23 mm length of 23 mm or solid spheres with 16 mm in diameter were used to strike 100 x 100 x 10 mm test targets. The impact velocities tried typically varying from 270 to 925 m/s. A finer mesh was applied to the target area close to the side face of impact to better capture the projectile-target interaction features. When the calculated and experimental data are compared, it found that the suggested model seems to do an excellent job of explaining how longitudinal elastic and transverse elastic waves propagate through the test objective after a strike and that the expected velocity of these elastic waves are reasonably equivalent to those observed in experiments. In terms of the time evolution of dimension and form of the convenient damage zone, it is a high convention with numerical and experimental data.

Peroni et al.[8] performed compression and splitting tensile tests between 10^{-3} and 10^{3} strain rate values of the glass specimen used in layered glass structures using SHPB. The research centered on understanding how deformation rate affects the tensile and compressive strength of glass. The young modulus, and ultimate strength are not strain rate dependent. There is a considerable rise in the ultimate tensile strength at high strain rates.

Zhang et al.[9] applied laboratory to research the dynamic mechanical characteristics of glass with annealed, which is commonly used in construction implementation. Young's modulus and strain rate on strength of glass are investigated. Due to measure the glass's static stress and elastic modulus, static testing was initially conducted. Dynamic compressive experiments, utilizing a modified SHPB, were then performed at rates of strain between 98/s and 376/s. Through a Brazilian tensile test, tension tests were carried out in the rate of strain between 35/s and 990/s. The results of the tests show that both tension and compression stress are extremely susceptible to the strain rate. The conclusions of compression tests show that the strain rate has a considerable impact on the compressive glass’s strength. According to the Brazilian tests data, the dynamic tension stress also increase strain. Also, elastic modulus of the glass material was not related to the strain rate.

Daryadel et al.[10] tested four different glass types, starphire, borosilicate, fused silica, and soda-lime in a drop weight test system and SHPB test system to examine their dynamic behavior and energy absorption capabilities. All glass types showed a similar pattern in the punch shear test at low impact velocities, however, borosilicate and starphire had the maximum total energy absorption. SHPB compression experiments were performed at two distinct strain rates. In comparison to the other glass types, borosilicate had greater absorption of energy, compressive stress, and failure strain. The SHPB compression results revealed a significant strain-rate dependency.

Zhang et al.[11] obtained the JH-2 material model parameters conducting quasi static compressive test and dynamic compressive tests on annealed soda-lime glass. First, cylindrical glass specimens with a radius of 7.5 mm were subjected to the quasi-static compression test with a strain rate of 1.33e-4 s^{-1}. Then, the brittle specimens were tested in the SHPB dynamic test system at rates of 619 s^{-1} and 1465 s^{-1}.

Sheikh et al.[12] performed static compression and dynamic compression tests on 8 mm cube-shaped, annealed, and chemically strengthened aluminosilicate glass specimens with a Universal testing machine and SHPB set-up. Although the surfaces of the annealed glass were imperfect and rough, the surface of chemically strengthened aluminosilicate glass was smooth and scratch-free. Although the material surfaces were different in both samples, it did not affect the static compression test results. Both annealed glass (AG) and chemically strengthened glass (CSG) demonstrated in the dynamic compression test that the compressive stress is strain rate dependent, and that the stress is substantially enhanced at high strain rates. CSG has an average compressive strength that is around 100 MPa greater than the AG compressive strength. Axial cracks in both glasses initiate the damage and lead to specimen failure.

Fu et al.[13] investigated the tensile behavior of polycarbonate using the Split Hopkinson Tensile Bar system. Results of dynamic and quasi static studies revealed that the tensile behavior of polycarbonate was dependent.

PVB is one of the most preferred interlayer material in the automotive industry, where layered glass systems are used due to their mechanical superior behavior. Xu et al.[14] performed load studies using SHPB at strain rates of 700 s^{-1}, 1200 s^{-1}, 2200 s^{-1}, 3500 s^{-1}, and 4500 s^{-1}. PVB deforms in two models: the compact phase and the hardening phase. The first is influenced by the strain-hardening effect, while the second is influenced by the stress-hardening effect. The Mooney-Rivlin Material Model was found to accurately capture the dynamic behavior.

Hu et al.[15] investigated the quasi static and dynamic compression characteristic of polycarbonate at different strain rates and temperatures. Pulse shaping was applied in the testing of polycarbonate using SHPB. The results indicated that polycarbonate is a temperature- and rate-dependent material, with yield stress increasing with strain rate and reducing with temperature.

Grant et al.[16] examined the fracture behavior of the layered glass structures with different glass thicknesses. The PVB thickness was kept constant in all systems. The thickness of glass varies between 0.7 mm and 2.5 mm. A 200 mm square plate was tested at perpendicular and 45-degree with impact velocities over the range of 4 m/s and 20 m/s. The measured velocity at the first damage in the layered glass structure was called the critical velocity. The protection efficiency was increased by increasing the thickness of the top glass and decreasing the thickness of the lower glass. As the thickness of the top glass increased, the radius of the cracks that generated within glass was also increased. On the plate with an angle of 45 degrees, a higher critical velocity was noted.

Zhao et al.[17] investigated penetration resistance of layered automobile glass exposed to head impact a continuum damage mechanics (CDM)-dependent model through FEA simulation. Initially, the PVB thickness was kept constant at 0.76 mm, and the total thickness of the two glasses was taken as 3.5- and 4-mm. Glass thicknesses were determined as 2x2 mm, 2.5x1.5 mm, 1.5x2 mm, and 2x1.5 mm for the four cases, respectively. The highest damage content was observed in the thinnest interlayer. The thicknesses of the PVB interlayer, was varied, consisting of 0.38-mm, 0.76-mm, and 1.52-mm thicknesses, respectively. The least damage occurred with the thickest PVB interlayer used. Square plates of 240 mm and 400 mm were analyzed to see the influence of plate size. Higher failure content in the plate with smaller dimensions was observed.

Timmel et al.[18] modeled the PVB interlayer by using Blatz-Ko material, Mooney-Rivlin material, and Ogden material model. Both a Blatz-Ko and Mooney Rivlin material models succesfuly simulate the constitutive behaviour of PVB.

Liu et al.[19] studied the energy absorption capability of PVB layered glass. A compression test was performed on a 2x2x0.76 mm thick, 12 mm diameter circular PVB layered glass sample in SHPB with a strain rate of 800/s. The impactor with the weight of a human head was hit to a plate consisting of automotive glass dimensions with a velocity of 25 m/s, 20 m/s, 15 m/s, 10 m/s, and 5 m/s, and an aspect of 0, 15, 30, and 45 degrees in sequence. The system absorbs more energy as the impactor speed increases,

but the amount of energy absorption decreases when the impact angle increases. In addition, a stress distribution on plate spreads circularly.

Xu et al.[20] conducted the quasi static and dynamic compression tests of a windshield structure. PVB laminated glass exhibits substantial strain-rate dependency and presented nonlinear effects under at both quasi static and dynamic applied loads.

Thompson et al.[21] performed the windshield head impact test both experimentally and numerically. For glass JH-2 and for PVB Simplified Rubber constitutive models were selected in the simulations.

Larcher et al.[22] investigated the behaviour of layered glass subjected to air blast load. To verify the correctness of the different material models and different model shapes were used in the simulations. The shell model, solid model, and smeared model were developed and compared with experimental data, and it was observed that the results matched each other.

Peng et al.[23] studied the dynamic deformation characteristics of glass panels. In their study, windshield models were created with various configurations of glass and PVB with several attachment techniques. All models were subjected to head impact. LS-DYNA was used for all simulation, and Laminated Glass Material Model was preferred. The models were categorized as single-layer glass, two layers of PVB and glass, and three-layer models with a single PVB layer between the two glasses. In addition, two different connecting methods were tried between layers: shared nodes and tied connections. Model results and test results were compared, and it was observed that the crack propagation in the component did not match well when compared with the test results.

Liu et al.[24] studied static and dynamic tests in the laboratory environment to determine the dynamic characteristics of the PVB interlayer. Quasi static tensile tests were applied with rates of $4x10^{-3}$/s, $2x10^{-2}$/s, and $8x10^{-2}$/s, and quasi static compression tests were applied at rates of $4x10^{-4}$/s, $4x10^{-3}$/s, and $4x10^{-2}$/s. The dynamic tensile test was performed at 118/s and the dynamic compression tests were performed at 1200/s–4500/s. When the compression test results of the PVB material were examined, material behaves in a viscoelastic manner at quasi-static loading, it exhibits elastoplastic behavior at dynamic rates.

Zhang et al.[25] investigated impact resistance of a PVB laminated glass system. In their study, a rectangular piece of wood with weights between 2 kg and 8 kg was hit the

layered glass plate at velocity between from 9 m/s and 35 m/s. Increasing the thickness of the PVB interlayer resulted increased penetration resistance.

Zhang and Hao investigated effect of the boundary conditions and interlayer anchorages of layered glass panels exposed to the blast loads both experimentally and numerically. Windshield samples with various frame thicknesses, movable or fixed ends, and interlayer anchorages were tried through blast testing. It was discovered that interlayer anchoring with fixture wire and fixture screws might successfully attenuate the laminated glass connection failure from moderate to high blast loadings. The PVB fracture potential is raised by strengthening the border anchoring [26].

Hidallana-Gamage et al.[27] studied different modeling methods to investigate the post crack behaviour of layered glass. The blast resistance of a layered glass panel is affected by the tensile strength (T) of the glass. As the glazed windows break under high blast loads, the PVB layer and its characteristics have a significant effect on how components respond to the explosion. While it has minimal effect on the characteristic of the layered glass when it is exposed to greater deformations under strong blast pressures, the rigidty of junction is reduced, increasing the flexibleness at the reinforcements, and reducing stress and failure to the glass layer.

Hidallana-Gamage et al.[28] investigated how interlayer characteristics affected the behavior of layered glass plates exposed to blast loads. The thicknesses of the PVB interlayer were determined as 2.28-mm, 1.9-mm, 1.52-mm, 1.14-mm, and 0.76-mm, respectively. In this work, the thickness and elastic modulus of the PVB were changed. As the interlayer thickness drops below a specific threshold, there is a dramatic rise in the maximum displacement.

Liu et al.[29] investigated the energy absorption system of PVB layered glass. Initially, a series of head impact studies on windshields were carried out at a range of impact velocities (6.6 m/s and 11.2 m/s) and impact angles (60° and 90°). The interlayer thickness has an important effect on the Head Injuriy Criteria value.

Li et al.[30] studied the tensile characteristics of the PVB using a customized SHPB with strain rates of 30–100 s^{-1}. It was observed that as strain rates increased, the tensile modulus of the PVB increased.

Peng et al.[31] investigated the fracture characteristics of layered glass. In the experimental tests were performed the windshield consisting of tempered glass and PVB was tested; a flexural, a quasi static tension, compressive test, and dynamic compression test. The Johnson-Holmquist ceramics material model constants were obtained and the

model succesfully captured the dynamic responses of windshields. The PVB material was modeled using the Mooney-Rivlin material model.

Prasongngen et al.[32] used the shared node approach to simulate the bond among PVB film and glass. This was done using the element deletion approach to incorporate crack movement. The head impact test and the layered glass impact model presented reasonable agreement.

Samieian et al.[33] investigated the bond between the glass and the polymer experimentally and through modeling at various testing speeds and temperatures. Tensile tests were carried out on the fractured laminated glass and PVB. To determine the bond fracture strength, these experiments were used in conjunction with fracture mechanics techniques. A numerical simulation model was created using this adhesion fracture strength to forecast the removal of the PVB from the glass. It is determined that the adhesion is undependent on the temperature at a steady-rate in the studied range of temperature (20 °C–60 °C). It was discovered that adhesion depends on loading rate at a certain temperature.

1.2. Scope of the Study

Layered glass is formed by combining at least two layers of glass with a polymer interlayer material under heat and pressure. When layered glass structures are exposed to external dynamic loads, even if the glass inside the structure is shattered, the polymer interlayer prevents the structure from disintegrating and bursting. Layered glass is generally used in the defense, automobile, and aircraft industries It is also an industrial product that is widely used in buildings because these structures with a transparent and aesthetic appearance provide insulation against sound and heat.

In experimental studies on laminated glass, it is not easy to determine stress and its distribution in the structure, the amount of energy released, deformation in the glass layers, and the rate of deceleration of the projectile speed. For this reason, numerical analyses are performed to better understand the dynamic compression characteristics of layered glasses and to investigate the variables are not easy to measure in experimental studies.

In this thesis, the dynamic compression characteristics of the layered glass system were numerically investigated using LS-Dyna[34]. First, SHPB numerical analyzes were

performed to investigate distribution of the stress in the structure. In the dynamic compression SHPB models, a layered glass sample with a diameter of 6 mm and a cylindrical geometry was used, consisting of a polymer interlayer between two glass layers. Two different polymer interlayer types consisting of PVB, and polycarbonate were tried and compared. The interlayer type and thickness were investigated based on the effect the stress distribution.

Later, projectile impact test was modeled consisting of a rigid material with a diameter of 8 mm, was thrown at different speeds into the PVB-layered glass structure with 150 mm side lengths. The thickness and different arrangement of the layers were tried by keeping the PVB thickness constant. In these numerical studies, the rate of deceleration, and the amount of eroded energy were calculated and compared for different configurations. The protection efficiency of the glass layer was determined.

In this thesis, mechanical properties, and production process of glass and polymer materials were explained in Chapter 2. In Chapter 3, the material models used in numerical studies were explained in detail, and information about the modeling stages of the layered glass structure was given. In Chapter 4, the conclusions of the numerical analyses were given. In Chapter 5, the model results were interpreted.

CHAPTER 2

MATERIAL STUDY

In this chapter, the historical development of glass and PVB materials comprising the layered glass structure, their use in the industry, production methods, and mechanical properties were given. In addition, Split Hopkinson Pressure Bar test was explained.

2.1. Glass and Its History

Glass is widely used material in automobile and defense industries. Historians and archaeologists claim that glass was discovered by the Egyptians about 5000 years ago, but the first glassmakers were from China[35]. A party of mariners from Phoenicia disembarked from boat and cooked dinner on a mid-seacoast using natural-soda (sodium-nitrate) like the fire, according to historical documents that date back to 5000 years ago. The first glass was discovered by the sailors after the fire had subsided. It was translucent and shiny and was created by a disproportionation between sodium-nitrate and grid on the coast[36] [37]. The Egyptians created several patterned bottles and cans and opaque colored non-transparent glass objects. Ancient Romans produced a variety of glass items with diverse forms in the first century by raising the temperature of burners and developing clear glass[36] . Then, during the Medieval Era, as Venice was at the head of her grandeur, glass manufacturing flourished in Italy and was considered a closely guarded secret[36] [37]. A Frenchman by the name of NAF created plate glass in 1688 that was bigger than what the Italians were producing, but the production procedure drove up the price of the glass. Due to the high cost of glass products, most people only owned a few items made of the material. When this was going on, costly stained glass was employed in locations that earned it, like churches and sacred buildings[35]. The first glassmaking machine was created in 1828 by a Frenchman by the name of Robin[37] The poor caliber of the machine's output, though, prevented it from being promoted. In 1900s, the American automobile fabricator Ford fabricated a windshield. After this production, America became a leader in the glass industry[38]. Beginning in the 1980s, it became a

leader in the Chinese glass industry and had a significant job in the development of layered glass[39].

2.1.1. Manufacturing of Glass

Layered glass structures are typically made from flat soda-lime glass. The glass is made using the float technique, which Pilkington developed in 1959 [40]. Molten glass is allowed to float in a bath of liquid tin [41]. The control of thickness of the float glass is done by controlling the withdrawal speed of the glass material from the tin. After the glass passes through the annealing section, which consists of a long tube, it is slowly cooled down [42, 43]. The controlled and slow annealing process is the most critical in the manufacture of glass because it removes the internal stresses in the glass material and prevents the strength of the glass material from decreasing. In the last stage, the glass is cut according to the determined criteria in the cutting section [42 44].

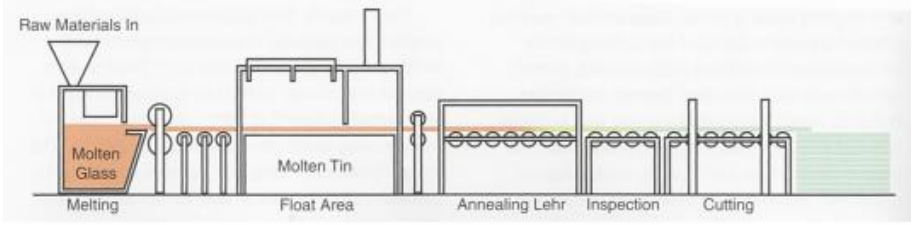

Figure 2.1 The glass process (Source: Patterson [42])

2.1.2. Type of Glass

Annealed-glass, heat-strengthened glass, and toughened-glass are the most used glass types in layered glass structures.

2.1.2.1. Annealed Glass

Glass is cut by scoring and snapping after being annealed, a procedure that gradually cools the glass to release internal tensions after it is made [45].

The glass is heated until the temperature reaches the safe stress zone. Although the glass is flexible enough to allow the tension to relax, it continues to be too rigid to

deform. Then, the glass is slowly cooled. Finally, the material is cut to the desired dimensions [46]. In fractured glass, sharp and pointed occurs on the broken edges of the glass [47].

Annealed glass exhibits elastic behaviour until fractured point. No creep and fatique behaviour were observed in the metallurgical investigations for annealed glass. Crack growth was slow in annealed glass, when it exposed to stress loading [48].

2.1.2.2. Heat-Strengthened Glass

There are procedures followed to make glass panels that improve the strength of annealed glass. The glass that has been heated has increased strength, impact resistance, and thermal stress resistance. Heat-treated glass is referred to as "annealed glass," which has undergone a controlled quick cooling process after being heated to a temperature close to its softening point [46].

The broken parts of heat-strengthened glass are larger than those of toughened glass. Used in layered glass system, large pieces of broken glass are preferred than those toughened glass. The reason is that the load-bearing capacity after breakage is better with large pieces of broken glass [47].

Heat-strengthed process is similar to the toughened process, but the pre-stress values formed in heat-strengthened glass are lower. Therefore, fraction occurs like annealed glass [49].

2.1.2.3. Toughened Glass

Float glass is heat treated up to 620 – 670 ˚C temparature ranges for the manufacture of toughened glass [47].

Toughened glass, also called tempered glass, creates surface and corner compression conditions in the heat treatment process. The surface of the heated glass is rapidly cooled. As the center of the glass cools, it exerts pressure on the surface and corners [46].

The bending strength value of toughened glass was increased due to a locked in compressive surface stress during heat treatment process [49].

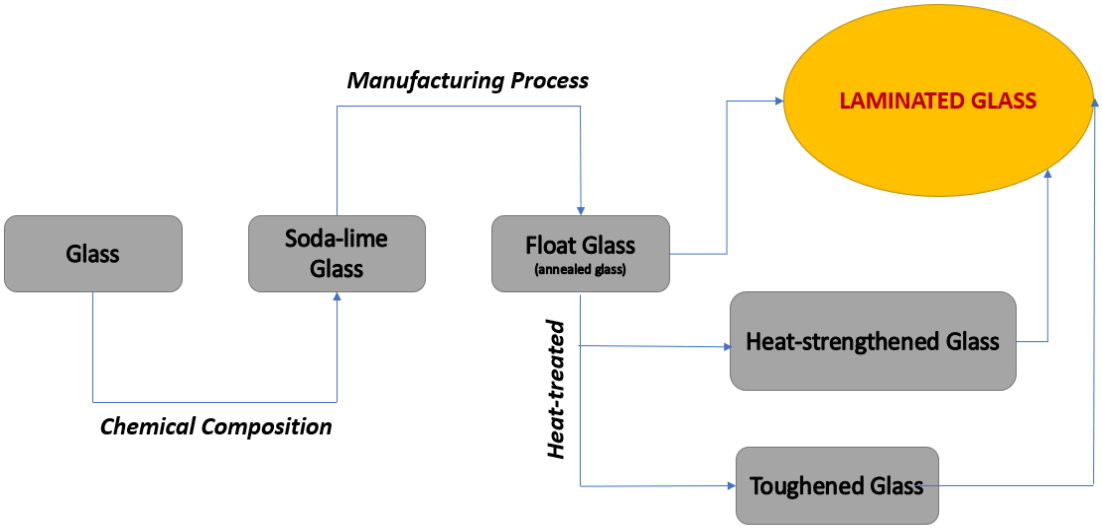

Figure 2.2 The steps of manufacturing of glass types

2.1.3. Mechanical Properties of Glass

Glass is a crystalline solid with an isotropic structure and brittle material behavior. While the glass subjected to stress loading deforms elastically, almost no plastic deformation is observed before breaking [50]. For this reason, the behavior of glass is elastic almost before fracture [47]. The compressive stress of glass is approximately 10 times greater than its tensile stress [43]. High-stress concentration occurs because the surface of the glass is flawed. It does not reduce the local stress concentration because of no plastic deformation [47].

2.2. Polyvinyl Butyral

Polyvinyl Butyral (PVB) interlayer is one of the material groups whose production increased after the First World War. Since the use of PVB in layered glass systems has increased rapidly for about 80 years, investors have been working on reducing the production cost of the material and eliminating the defects material. With the increasing use of PVB as an interlayer in car windows and safety glasses, research has been carried out on the improvement of sound insulation, sunlight transmission, and structural behavior [51].

In the 1930s, PVB was the preliminary substance utilized as an interlayer for layered glass. It is created when polyvinyl alcohol and butyraldehyde combine. PVB is a terpolymer with an amorphous structure, and PVB is available as vinyl-butyral (75–81 wt%) (x), vinyl-alcohol (17–23 wt%) (y), and vinyl-acetate (1.1–2.1 wt%) (z), which provide certain properties. It has three different monomers called monomers behavior [52, 53].

The PVB provides good mechanical and optical properties, including development mechanical stress, high deformation previously breaking, strong adherence to glass, and maximum sunshine transmission [54].

2.2.1. Mechanical Properties of PVB Interlayer

PVB is considered a linear elastic material and an incompressible [55].

PVB is among the plastic material groups. When the PVB material is subjected to compressive and tensile loads, it depends on the strain rate. Although PVB exhibits viscoelastic behavior with tensile quasi-static stresses, it exhibits elastoplastic behavior with dynamic tensile loading. It exhibits viscoelastic behavior in the compression scenario under dynamic and quasi-static loads [24].

When the tensile test is applied to the PVB material at different strain rates, a wide variation is observed in the stress strain values. This behaviour is caused the offset connection with fracture toughness and depends on the hardness and critical loadings of the PVB [56].

2.3. Polycarbonate

The unique and very practical category of high-heat polymers known as polycarbonates is noted for their hardness and transparency. The polycarbonates, which make them ideal for several applications, include high strength, transparency, light color, resilience to fire, and conservation of mechanical properties across a large temperature range. Polycarbonate material acts as an intermediate layer in layered glass systems since it is approximately 250 times more resistant to impacts than glass and has a transparent nature [46].

Polycarbonate is used in security systems with glass and has the potential to stop bullets because it deforms upon contact with a bullet and absorbs the energy of the bullet. Even if the glass shatters when the laminated glass is exposed to the bullet, the polycarbonate can damage and stop the impactor, preventing the layered glass system from being punctured [57].

2.4. Layered Glass

Laminated glass is one of the widely used materials in the automotive, aircraft, defense, and construction industries. Layered glass is formed by connecting two or more glasses with polymer interlayer material at high pressure and heat (140 °C) [40 42]. It has a safe, sound-insulating, and heat-resistant structure [42 47]. Because of the polymer interlayer, laminated glass has greater resistance to sudden load sources like gunshots and explosive loads [42 47]. Laminated glass is preferred in engineering materials since laminating improves the post-failure behavior [47]. The interlayer's function is to keep the broken pieces together, and to reduce the chance of glass fragment injuries. Laminated glass is produced with glass types and thicknesses, such as annealed-glass, heat treated glass, and toughened glass, and in different polymer types and thicknesses, such as PVB, polycarbonate, EVA, SPG, and TPU [44].

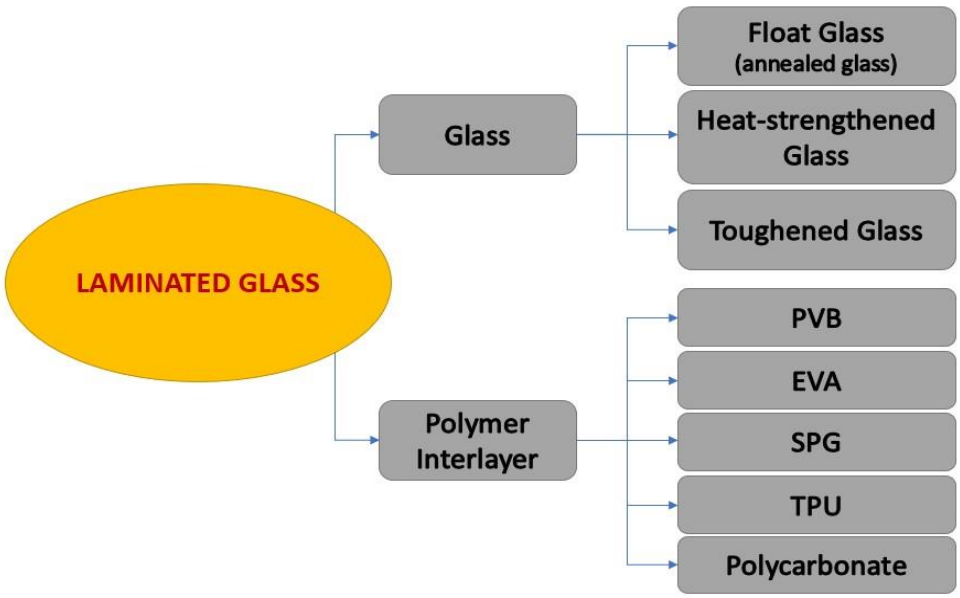

Figure 2.3 Constituent of laminated glass

2.4.1. Manufacturing of Layered Glass

Laminated glass is produced by two different methods: a dry procedure and the wet procedure.

2.4.1.1. Dry Method

The dry procedure applied in the production of layered glass is a production process consisting of 5 stages: cutting, laminating, pre-pressing, high-pressure kettle processing, and edge cutting [58].

During the cutting process, the glass plate is grinded from four corners by the grinding machine. Before the laminating process, the PVB material is cut a little more than the glass dimensions, and this process should be done with room temperature and humidity between 18 and 28 percent in order not to decrease the strength value of PVB [59]. After cleaning the glass surface with a vacuum cleaner, two particles of glass and the PVB interlayer are vacuumed at a temperature close to 150 °C [58]. The purpose of prepressing layered glass, which is essential to the qualification of component, is to release air from the space where the glass panel and PVB are connected [58]. Layered glass production requires high pressure process. The performance of layered glass also depends on the parameters of temperature, pressure, and time. Glass for pressing must be heated and cooled at a slow rate [58]. In the edge-cutting process, the excess parts on the edge of the PVB are cut manually and equalized with the glass size [38].

2.4.1.2. Wet Method

After cutting, edging, and washing, raw glass layers are bonded; the layers must not be wet and surface dirty. The wet method is the period of folding glass and PVB. Glass layers must be bonded to form a cavity between them for grouting to complete the wet technique of lamination. Clustered liquid is injected inside the hollow throughout grouting, and PVB sheets are used to close the hollow's entrance [60].

2.4.2. Post-breakage Characteristics of Layered Glass

The post-breakage behaviors of layered glass and monolithic glass were compared. Depending on the empirical consequence, the behaviour was divided into three categories. Compressive and tensile stresses occurred in the lower and upper glass, which will be the first in the next stage. In the lower glass, fractures began to occur, but only the upper glass had compression and tensile stresses. In the last stage, although the upper glass started to break due to compression stress in the upper glass and tensile stress in the interlayer, the interlayer material prevented the broken glass pieces from dispersing. In other words, although the glasses were broken, the interlayer material was able to handle the loading [61].

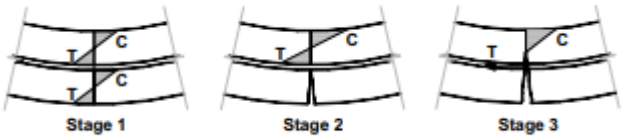

Figure 2.4 The post-breakage stress distribution of laminated glass (Source:Kott et al.[61])

The degree of glass fragmentation, for example, and the kind of interlayer employed as well as the tempering method utilized affect the load-bearing performance that remains after fracture. Greater post-break behavior of the laminated glass is caused by large pieces. Tempered glass's post-failure performance is less favorable than that of annealed glass due to its fracture pattern with extremely small fragments. In this situation, the post-breakage ability exclusively based on the tension stress of the interlayer since tempered glass would droop like a hand towel. As a result, the qualities of stiffness and tensile strength are crucial for post-breakage mechanical capability [47, 62].

Figure 2.5 Fracture model: annealed-glass, heat strengthened glass, and toughened glass (Source: Haldimann et al.[47])

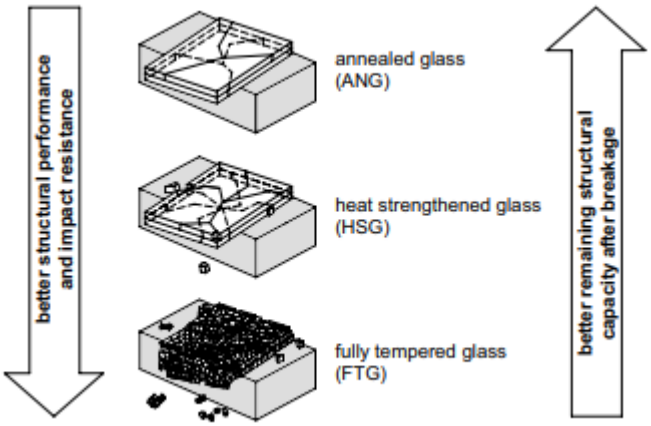

Figure 2.6 Post-breakage behavior of laminated glass made of different glass types (Source: Sedlacek et al.[62])

2.5. Split Hopkinson Pressure Bar Theory

The Split Hopkinson Pressure Bar is a dynamic test system providing dynamic stress strain behaviour out high strain rates. Device has three bars: striker, incident, and transmitter. The sample is sandwiched among the incident and the transmitter bars, and the striker bar hits the incident bar. An elastic compressive wave is generated when the striker bar hits the incident bar. This wave is called the incident wave ε_i (t). A portion of the compressive incident wave is reflected as it reaches the sample. The reflected wave ε_r(t) is the reflected portional of the wave due to impedence mismatch. The reflected wave is tension. The remainder of the compressive incident wave is transmitted to the transmitter bar, as compression, and it is called the transmitter wave ε_t (t).

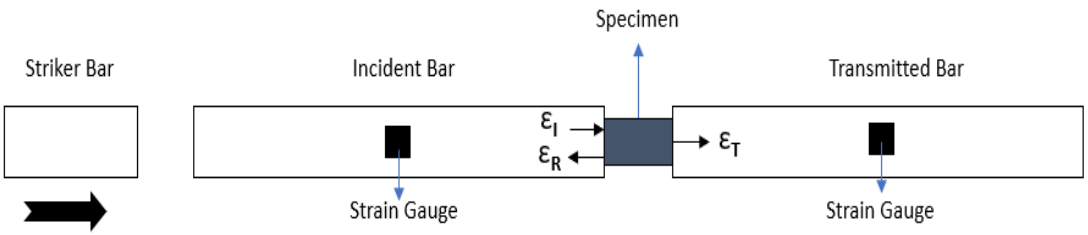

Figure 2.7 Stress wave propagation in SHPB

Strain values of ε_i ,and ε_r , are determined on the incident bar while ε_t is determined on the transmitter bar. The stress σ_s, strain ε_s, and strain rate $\dot{\varepsilon}_s$ of the sample were using the equation.

$$\varepsilon_s(t) = -\frac{2C_b}{L_s}\int_0^t \varepsilon_R(t)dt \tag{2.1}$$

$$\sigma_s(t) = \frac{A_b}{A_s}E_b\varepsilon_T(t) \tag{2.2}$$

$$\dot{\varepsilon}_s(t) = -\frac{2C_b}{L_s}\varepsilon_R(t) \tag{2.3}$$

where L_s is the length of the specimen, A_b is the cross-sectional area of bar, A_s is the cross-sectional area of the sample, E_b is the young's module of the bar, C_b is the wave velocity of the bar, and t is the time [63].

CHAPTER 3

NUMERICAL STUDY

LSDYNA is an implicit and explicit finite element method software program in which nonlinear structural simulations are applied to high structural deformations such as drop tests, impact, and penetration. The material model library, the ability to define contact formulations and a solution algorithm with its controls that analyzes complex models enables it to be used in the automotive, defense, and aerospace industries [34].

Although there are previously published experimental studies to examine the dynamic compression characteristics of layered glass systems, the number of numerical studies relatively less. The researchers generally preferred to use the Johnson-Holmquist Ceramics material model in these studies. For the PVB interlayer, material models exhibiting elastic, viscoelastic, hyperelastic, and elastoplastic behaviour were used.

In this thesis, the dynamic compression characteristics of the layered glass system were investigated modeling the SHPB and plate impact tests using LSDYNA. For glass, the Johnson-Holmquist material model and for the PVB interlayer material, the Ogden-Rubber material models were used. The SAMP-1 material model was used for the Polycarbonate.

In numerical studies, two different interlayer types (PVB and Polycarbonate) were used for the layered glass system in Split Hopkinson Pressure Bar models. PVB and polycarbonate interlayers with different thicknesses were modeled and their effects on stress wave propagation were compared. PVB was also used in penetration test models then different impact velocities and glass thickness combinations were tried. Resultant impact velocity of the penetration, eroded energy of layered glass system was compared.

3.1. Material Models

The Johnson-Holmquist material model for the glass layer, Ogden Rubber material model for the PVB interlayer, and the SAMP-1 for the polycarbonate interlayer were used in LSDYNA to investigate the dynamic compression characteristics of the layered glass system.

3.1.1. Johnson Holmquist Ceramics Material Model

The plasticity damage model developed by Johnson and Holmquist is convenient for modeling brittle materials like glass and ceramics. An article by Johnson and Holmquist has a more detailed definition of the material model [64].

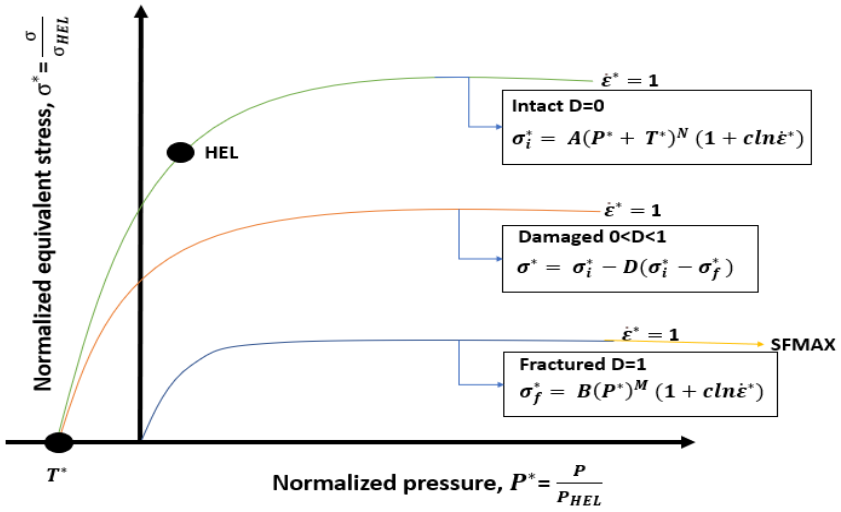

Figure 3.1 The strength of the JH-2

The normalized equivalent stress σ^* in the Johnson-Holmquist Ceramics material model represent is given by the following equation Figure 3.1,

$$\sigma^* = \frac{\sigma}{\sigma_{HEL}} \tag{3.1}$$

$$\sigma^* = \sigma_i^* - D(\sigma_i^* - \sigma_f^*) \tag{3.2}$$

Where σ_i^* is the normalized intact strength, σ_f^* is the normalized fracture strength. The normalized intact strength and the normalized fracture strength are given below,

$$\sigma_i^* = \frac{\sigma_i}{\sigma_{HEL}} \tag{3.3}$$

$$\sigma_i^* = A(P^* + T^*)^N (1 + c ln\dot{\varepsilon}^*) \tag{3.4}$$

$$\sigma_f^* = \frac{\sigma_f}{\sigma_{HEL}} \tag{3.5}$$

$$\sigma_f^* = B(P^*)^M\,(1 + cln\dot{\varepsilon}^*) \tag{3.6}$$

Where P^* is the normalized pressure, T^* is the normalized tensile strength, $\dot{\varepsilon}^*$ is the normalized strain rate. The normalized pressure, the normalized tensile strength, and the normalized strain tate are given in the equation as,

$$P^* = \frac{P}{P_{HEL}} \tag{3.7}$$

$$T^* = \frac{T}{T_{HEL}} \tag{3.8}$$

$$\dot{\varepsilon}^* = \frac{\dot{\varepsilon}^*}{\dot{\varepsilon}^*_{REF}} \tag{3.9}$$

A, C, N and B are the material constants.

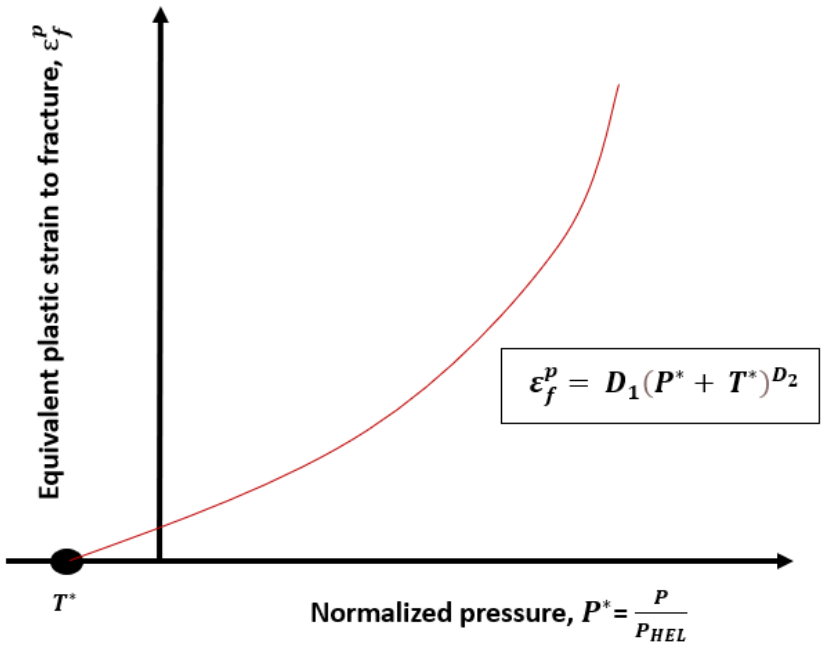

Figure 3.2 The damage model of the JH-2

Plastic strain to fracture increases as hydrostatic pressure increases Figure 3.2.

$$\varepsilon_f^p = D_1(P^* + T^*)^{D_2} \tag{3.10}$$

D_1 and D_2 are the damage parameters of the material. When the normalized pressure equals the normalized tensile strength, the material cannot undergo plastic strain.

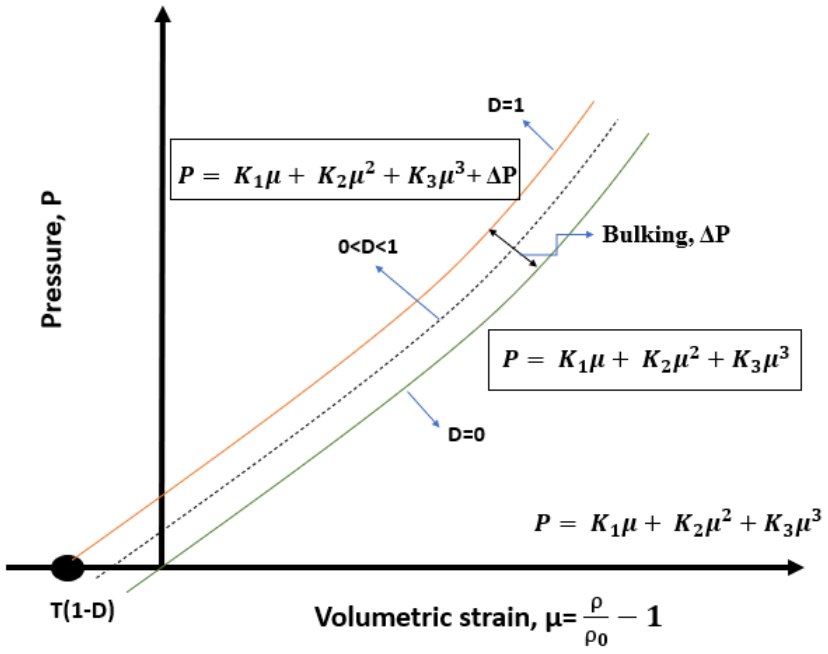

Figure 3.3 The pressure model of the JH-2

Figure 3.3 depict the JH-2 model's pressure vs. volumetric strain variation. The pressure is given by the following equation,

$$P = K_1\mu + K_2\mu^2 + K_3\mu^3 \tag{3.11}$$

where K_1, K_2, and K_3 are the constants, K_1 is the bulk modulus and μ is the volumetric strain given by $\mu = \rho/\rho_0 - 1$ where ρ and ρ_0 are the density and initial density, respectively. The tension is $\mu < 0$, the hydrostatic pressure is $P = K_1\mu$. After damage starts (D>0), bulking occurs. Hydrostatic potential energy is created from a portion of the elastic energy loss (pressure). HEL, G, and μ_{HEL} are determined from the following equation [34].

$$HEL = K_1\mu_{HEL} + K_2\mu_{HEL}^2 + K_3\mu_{HEL}^3 + \frac{4}{3}G\left(\frac{\mu_{HEL}}{1+\mu_{HEL}}\right) \tag{3.12}$$

$$P_{HEL} = K_1\mu_{HEL} + K_2\mu_{HEL}^2 + K_3\mu_{HEL}^3 \quad (3.13)$$

$$\sigma_{HEL} = 1.5(HEL - \rho_{HEL}) \quad (3.14)$$

The definition of the variables in the Johnson-Holmquist ceramics material model is as follows [34]:

- RO = Density
- G = Shear modulus
- A = Intact normalised strength
- B = Fractured normalised strength
- C = Strength constant (for strain rate dependent)
- M = Fractured strength constant (pressure exponent)
- N = Intact strength constant (pressure exponent)
- EPS0 = Quasi static threshold strain rate
- T = Maximum tension pressure strength
- SFMAX = Maximum normalised fractured strength
- HEL = Hugoniot elastic limit
- P_{HEL} = Pressure component at Hugoniot elastic limit
- σ_{HEL} = Strength component at Hugoniot elastic limit
- BETA = Fraction of elastic energy loss transformed to hydrostatic energy.
- D_1 = Constant for a permanent strain to fracture
- D_2 = Constant for a permanent to fracture (exponent)
- K_1 = 1st pressure factor (equivalent to the bulk modulus)
- K_2 = 2nd pressure factor
- K_3 = 3rd pressure factor
- FS = Failure strain

3.1.2. Ogden Rubber Material Model

Ogden Rubber material model was used for the PVB interlayer. PVB is nearly incompressible due to bulk modulus is significantly greater than the shear modulus. A

hydrostatics work component is added to energy of the strain function, which is a function of the relative volume, J, to model the rubber as an unrestricted material [65].

$$W^* = \sum_{i=1}^{3} \sum_{j=1}^{n} \frac{\mu_i}{\alpha_j} \left(\lambda_i^{*\alpha j} - 1\right) + K(J - 1 - LNJ) \tag{3.15}$$

The asterisks (*) remarks that the volumetrics effects were removed from the major stretches, λ_j^*. An integral convolution of the following kind is used to account for rate effects in linear viscoelasticity:

$$\sigma_{ij} = \int_0^t g_{ijkl}(t - \tau) \frac{\partial y^{\varepsilon kl}}{\partial x_\tau} \, d\tau \tag{3.16}$$

S_{ij} is the term for the second Piola-Kirchoff stress and E_{ij} is the term for the strain tensor of Green.

$$S_{ij} = \int_0^t G_{ijkl}(t - \tau) \frac{\partial y^{Ekl}}{\partial x_\tau} \, d\tau \tag{3.17}$$

$g_{ijkl}(t - \tau)$ and $G_{ijkl}(t - \tau)$ are the function for varied stress value. This stress is applied to the stress calculated using the energy of strain function. Six nominals from the Prony series serve as the representative for the function if it simply wants to incorporate basic rate effect:

$$g(t) = \alpha_0 + \sum_{m=1}^{N} \alpha_m e^{-\beta t} \tag{3.18}$$

$$g(t) = \sum_{m=1}^{n} G_i e^{-\beta t} \tag{3.19}$$

where G_i is the shear moduli, and β_i is the decay constant. This system, consisting of a sequence of dampers and springs, it come out of a sequence of dampers and springs and is a Maxwell fluid. Shear moduli and decay constants are used to describe this in the input. It is optional to include viscoelastic properties, and any term count may be employed. This viscoelastic expression avoids a constant shear modulus by only

including a term in the sequence when $\beta_i > 0$. For VFLAG = 1, the viscoelastics formula is,

$$\sigma_{ij} = \int_0^t g_{ijkl}(t-\tau)\frac{\partial y^{\sigma_{kl}^E}}{\partial x_\tau} d\tau \tag{3.20}$$

where σ_{kl}^E is the instantaneous stress appreciated from the internal energy functional. So, rather than elastic moduli, the values in the prony series relate to normalised relaxation modulus [34].

3.1.3. SAMP-1 Material Model

This material model was developed by Kolling, Haufe, Feutch, and Du Bois [66].

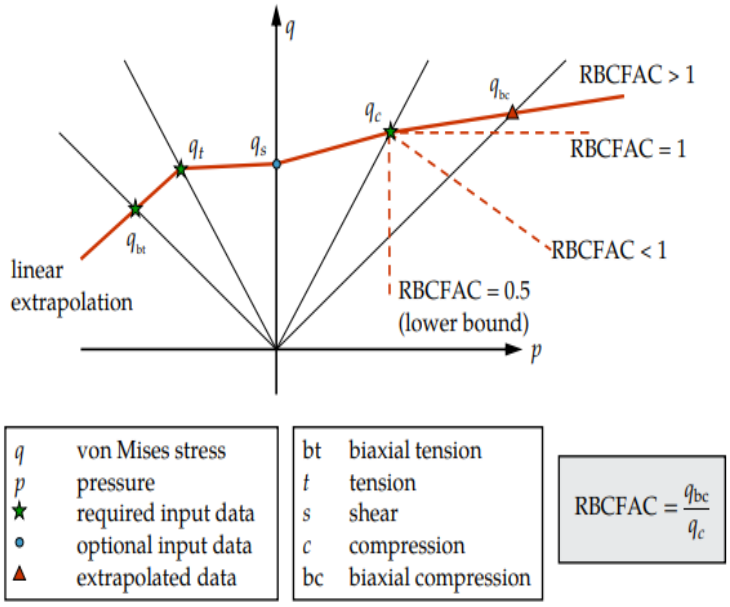

Figure 3.4 Von-Mises stress (Source: LS-DYNA[34])

In the event of no more than three load curve, a lineary yields surface in the affine cavity bounded by the von-mises stress and the pressure is produced taking the information at hand [34].

A damage curve because of comparable permanent strain occurring above the stress is generated if the LCID-D is provided.

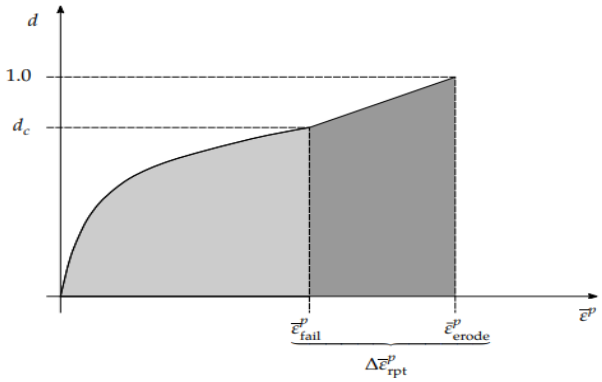

Figure 3.5 EPFAIL and DEPRPT described the failure and damped behaviour of a single element (Source: LS-DYNA[34])

Fundamentally, Material SAMP-1 evaluates a quadratic yield surface using three yield curves. The four types of yield curves that SAMP-1 takes are LCID-T (uniaxial tensile test), LCID-C (uniaxial compression test), LCID-S (shear test), and LCID-B (biaxial test); only LCID-T requires data from tension testing; the other three are available. The remaining curves are structured if less than three curve are specified, as shown by assigning the deficient load curve Ids to 0 [34].

3.2. Single Element Analysis

The PVB interlayer in the layered glass systems was used in both SHPB and projectile impact models. In Ogden Rubber Model for the stress and strain input provided from the experimental test was entered LSDYNA as input. Single-element analysis was done using LSDYNA to examine the consistency of the parameters.

Experimental dynamic compression and dynamic tension stress-strain data were taken from the study by Xu et al.[14] and Liu et al.[24] experimentally measured the mechanical behaviour of PVB material used in automotive impact windshield studies under dynamic compression loading in the SHPB system. By fitting the stress/strain data with various strain rates obtained from SHPB to a stress-strain curve suitable for the Ogden Model was obtained Xu et al. [14] and Liu et al. [24].

The stress and strain graph supplied from the uniaxial dynamic tension test results required for the PVB material was also taken from the study by Iwasaki [56]. Liu,

furthermore, adapted the stress and strain curve of this dynamic tensile test result and rearranged it for use in numerical models [24].

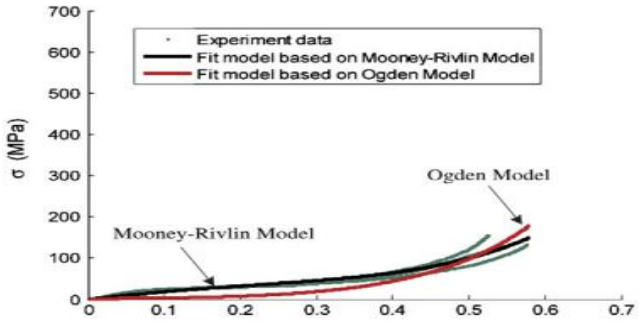

Figure 3.6 Dynamic-compression test at strain rate of 700/s for PVB
(Source: Xu et al. [14])

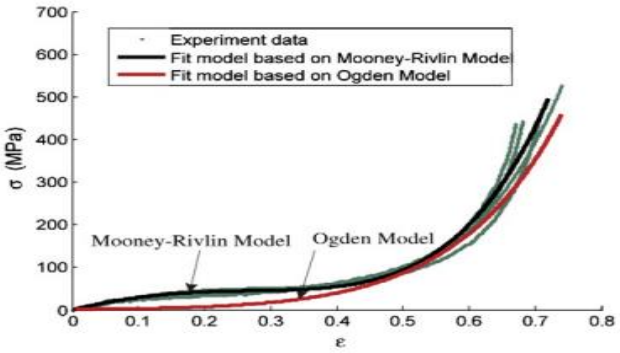

Figure 3.7 Dynamic-compression test at strain rate of 4500/s for PVB
(Source: Xu et al. [14])

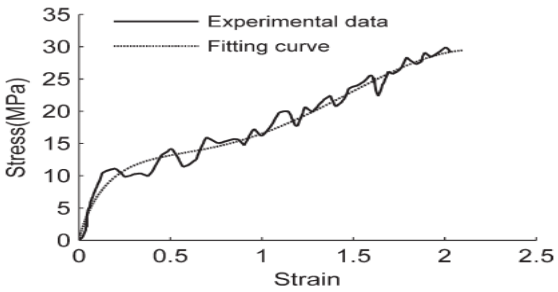

Figure 3.8 Dynamic-tension test at strain rate of 118/s for PVB
(Source: Liu et al.[24] Iwasaki et al.[56])

PVB single element model with a size of 0.25 mm were located in LSDYNA under both compression and tension up to the displacement value of 60% of total height as shown in Figure 3.9. Previously mentioned stress strain curves were entered as input.

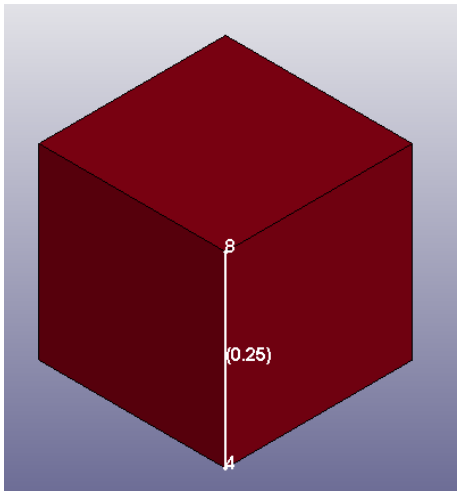

Figure 3.9 PVB single-element model

The number of terms in fit (NV value), which is one of the parameters in the Ogden Rubber material card, is set to 6 by default. The order of fit to the Ogden model (N) constant was taken as 3, 6 and 8, respectively. Models were rerun then stress-strain data were analyzed for rates of 700/s compression, 4500/s compression, and 118/s tension. The description of the parameters of the analyzed models is summarized in Table 3.1.

The fit from the d3hsp file is expressed in stretch and engineering stress values. The stretch was converted into engineering strain ($\lambda=1+\varepsilon_e$). The data obtained from the d3hsp file N: 3, 6, and 8 values were compared with the experimental curve. The results of the experimental and numerical for the PVB are in good correspondence with each other. The results of the single element analysis for PVB are given in Figure 3.10 to 3.14.

A similar study was also carried out for polycarbonate as well. The SAMP-1 was choosed as the material model. The experimental stress-strain data required for the material card, dynamic compression results at $0.001s^{-1}$ strain rate [15], and dynamic tension results at $0.001s^{-1}$ and $1750s^{-1}$ strain rates in Figure 3.15 [16], are defined as input.

The results of the experimental and numerical studies for the PC do match each other to some extend. The result of this study is given Figure 3.16.

Table 3.1 The description of the parameters used in the models for the PVB single element using Ogden Rubber Model

Model No	Strain Rate and Analysis Type	N Value
1	700/s Compression	3
2	700/s Compression	6
3	700/s Compression	8
4	4500/s Compression	3
5	4500/s Compression	6
6	4500/s Compression	8
7	118/ Tension	3
8	118/ Tension	6
9	118/ Tension	8
10	700/s - 118/s Compression	3
11	700/s - 118/s Compression	6
12	700/s - 118/s Compression	8
13	4500/s - 118/s Compression	3
14	4500/s - 118/s Compression	6
15	4500/s - 118/s Compression	8

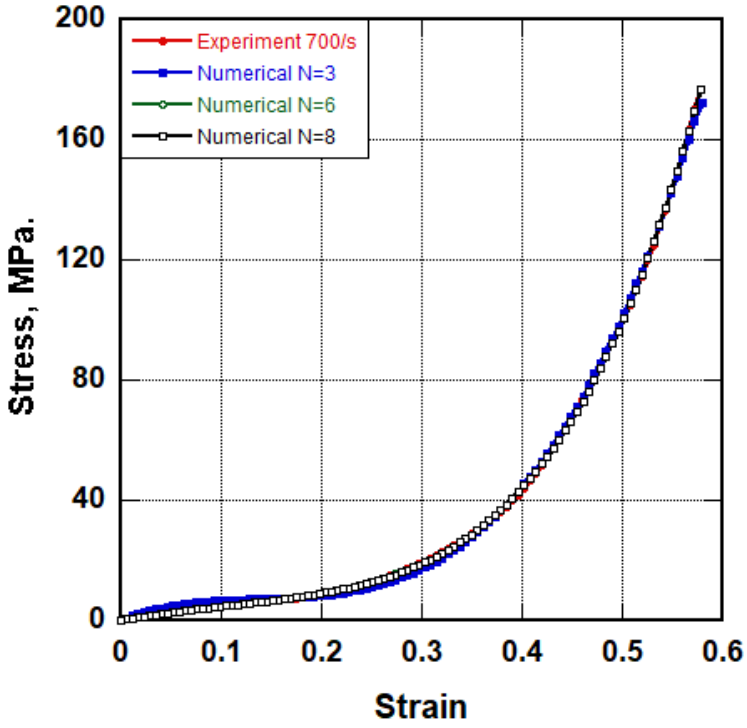

Figure 3.10 Compression engineering stress-strain curve at 700/s

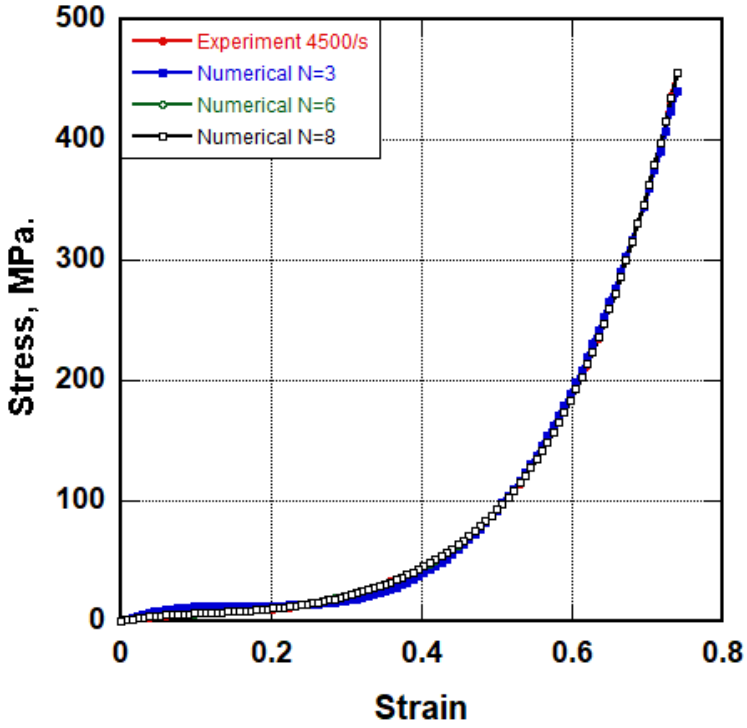

Figure 3.11 Compression engineering stress-strain curve at 4500/s

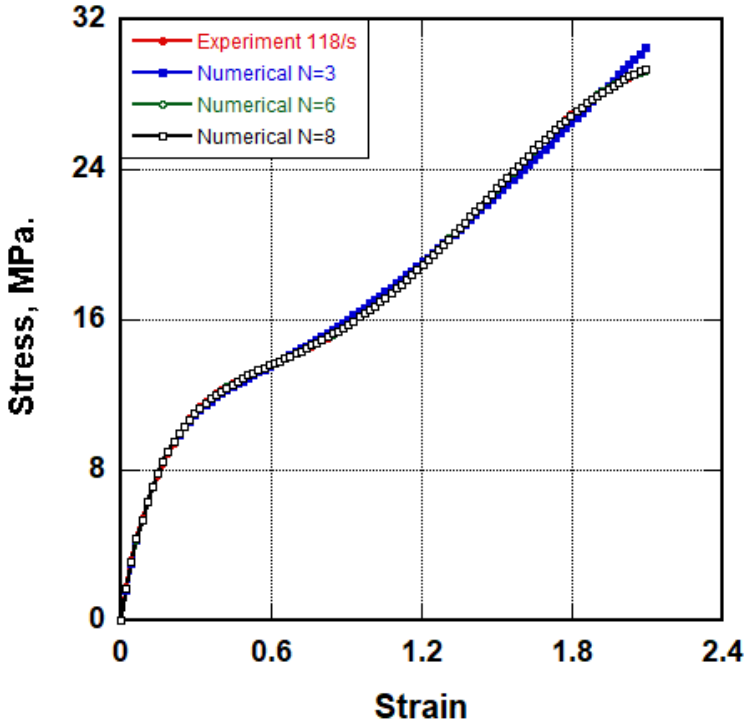

Figure 3.12 Tension engineering stress-strain curve at 118/s

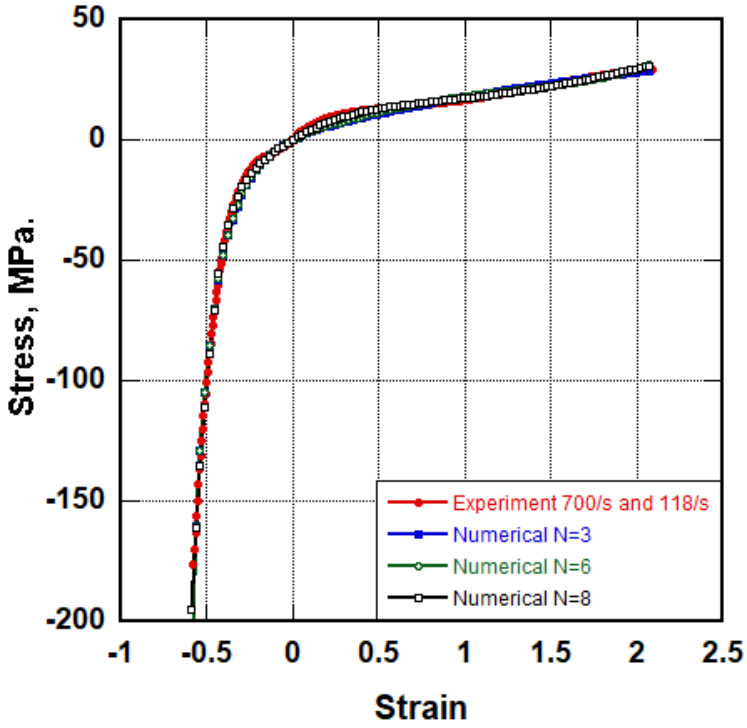

Figure 3.13 Compression and tension engineering stress-strain curve at 700/s and 118/s

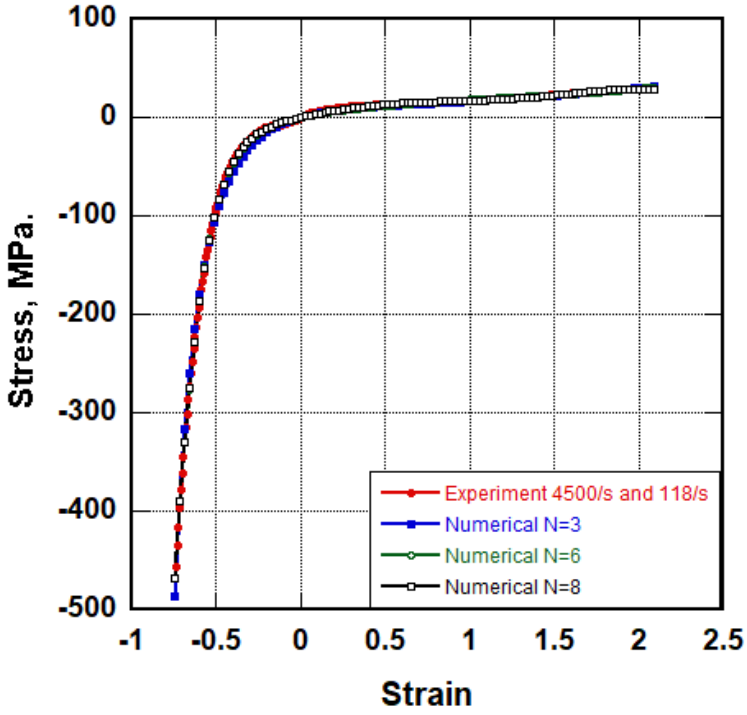

Figure 3.14 Compression and tension engineering stress-strain curve at 4500/s and 118/s

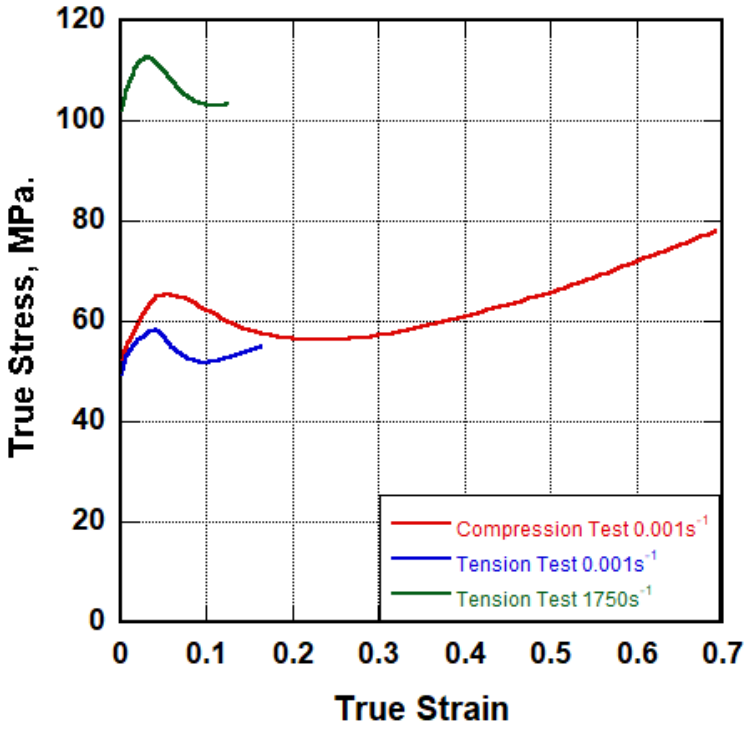

Figure 3.15 Test input curve for PC single-element model

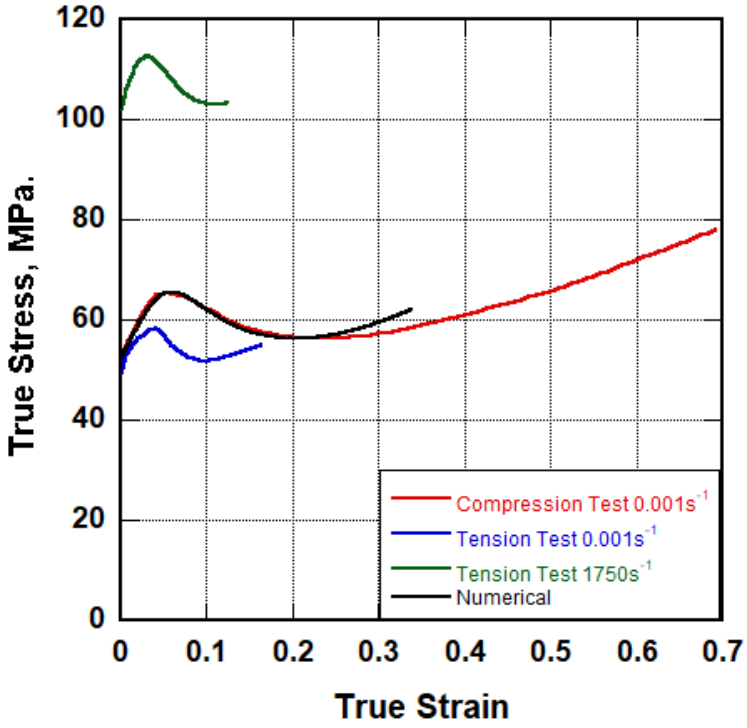

Figure 3.16 PC single-element model

3.3. SHPB Numerical Model

In this section, a stress wave propagation study was carried out by modeling the Split Hopkinson Pressure Bar of a layered glass system.

In this thesis, SHPB simulations were done for a layered glass system consisting of a polymer interlayer between two glass layers. The stress distributions for two different interlayer materials (PVB and PC) were then compared. The thickness of the top glass part and bottom glass part is 2mm, and the thicknesses of the PVB and PC interlayers are selected as 0.38 mm, 0.56 mm, 0.76 mm, 1.14 mm, 1.52 mm, and 2.28 mm. The diameter of the layered glass sample is 6 mm. The isometric views of the laminated glass specimens are given in Figure 3.17.

Figures a, b, c, d, e, and f represent the different thicknesses of the polymer interlayer, 0.38 mm, 0.56 mm, 0.76 mm, 1.14 mm, 1.52 mm, and 2.28 mm.

JH-2 material model constants are taken from the study by Holmquist et al. [67] and given in Table 3.2. In Figure 3.18, The sample/bar interfaces of the SHPB model are given.

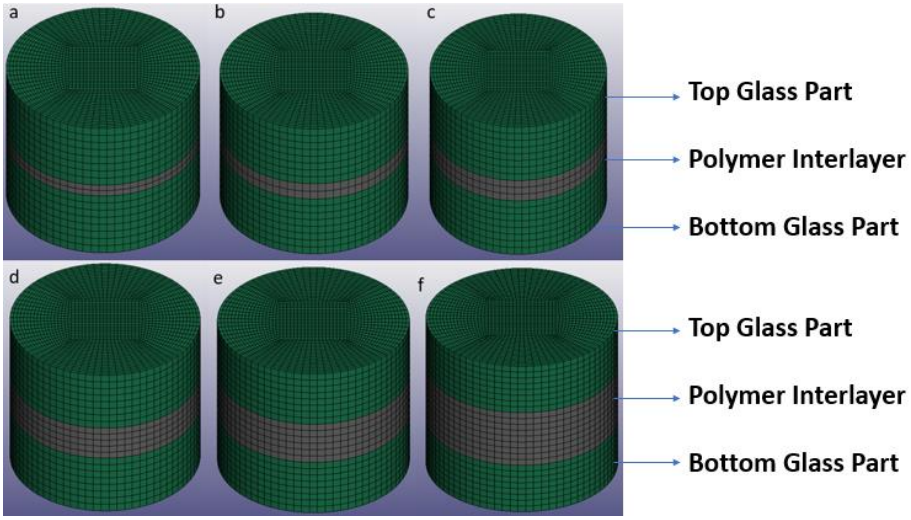

Figure 3.17 The isometric views of the laminated glass samples

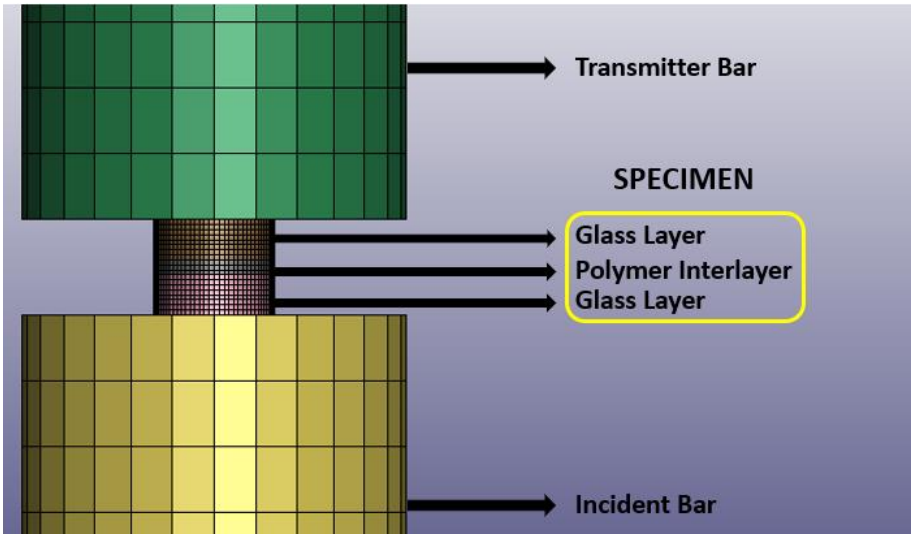

Figure 3.18 The sample/bar interfaces of the SHPB model in the LS-DYNA

Despite the presence of a striker bar in the SHPB test system, no striker bar was used in the modeling. Instead, the pressure-time data provided from previous tests were defined in curve. This pressure history was defined to the incident bar end. A typical SHPB set up used in dynamic testing and modeling laboratory of the department of mechanical engineering at the Izmir Institute of Technology, can be seen in Figure 3.19. Experimentally obtained incident pulse data is given in Figure 3.20.

Table 3.2 JH-2 values of soda-lime glass [67]

JH-2 Parameters for soda-lime glass	Value
Density (kg/m^3)	2530
Shear Modulus (GPa)	30.4
A	0.93
B	0.088
C	0.003
M	0.35
N	0.77
Ref Strain Rate	1.0
Tensile Strength (GPa)	0.15
Normalized Fracture Strength	0.5
HEL (GPa)	5.95
HEL Pressure (GPa)	2.92
HEL Strength (GPa)	4.5
D_1	0.053
D_2	0.85
K_1 (GPa)	45.4
K_2 (GPa)	-138
K_3 (GPa)	290
Beta	1.0

Figure 3.19 SHPB test system

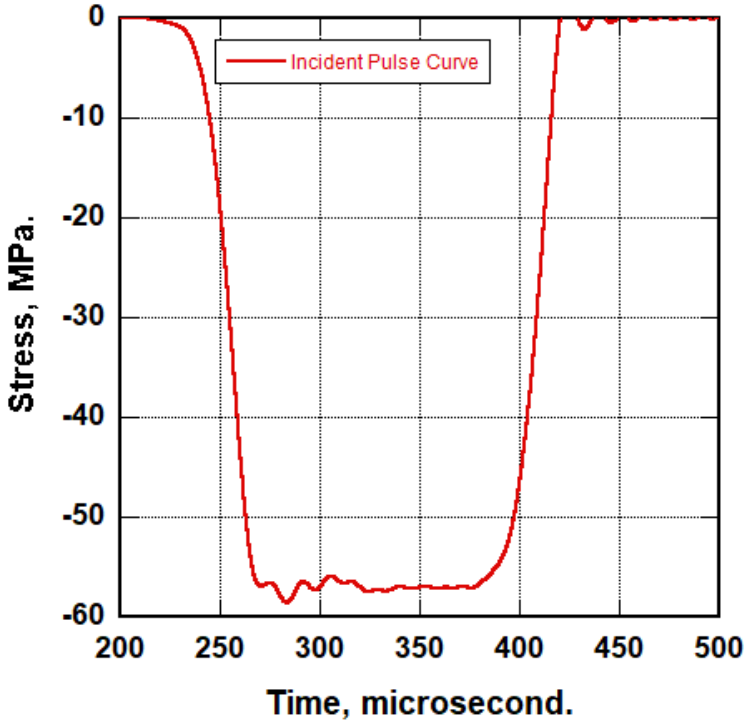

Figure 3.20 Experimentally determined incident wave

A perfect bond between the glass and interlayer surfaces was defined Automatic surface to surface contact types were used among the other layers. In Chapter 4, numerical results are given in detail.

3.4. Projectile Impact Numerical Model

In this study, a square-shaped PVB layered glass plate with a side length of 150-mm was analyzed using LSDYNA at different thicknesses, configurations, and impact velocities. The purpose is to compare different PVB-layered glass configurations and, to determine the deceleration rate, to determine the amount of eroded energy in layered glass, and to examine the energy balance in the components. The same material cards used for the glass layer and PVB interlayer in the SHPB models were also used in the projectile impact models. Detailed explanations about material cards are given in section 3.4. For JH-2 material model fail if damage strength was activated by assuming FS value as -1 and the Erosion card for the Ogden Rubber material card was determined with maximum principal strain value of was 0.75. A 4 mm radius a ball-shaped stainless-steel impactor was used in the analyses. The Elastic material model was chosen for the impactor.

2-Layer, 3-Layer, and 4-Layer systems were designed. The constituents of these systems are as follows: 1 PVB interlayer between 2 glass layers, 2 PVB interlayers between 3 glass layers, a total of 2 PVB interlayers between each glass one by one, and a total of 3 PVB interlayers between 4 glass layers were placed between each glass one by one. The thickness of each glass is 2 mm, and thickness of each PVB film is 0.76 mm. The layered glass structures were shot at 100 m/s, 150 m/s, 200 m/s, 250 m/s, 300 m/s, 350 m/s, 400 m/s, 450 m/s, and 500 m/s. The configurations of the systems are displayed in Figure 3.21.

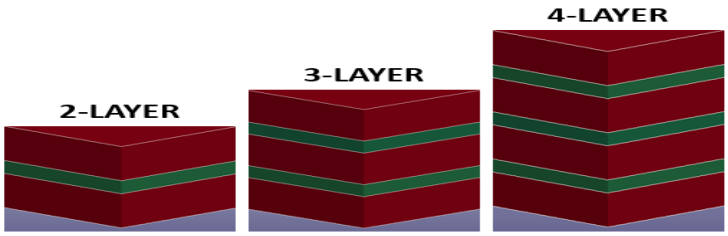

Figure 3.21 Different configurations tried as layered glass system

Also, a single PVB interlayer system between the two glass layers was designed with a total glass thickness of 3 mm, 4 mm, and 5 mm. These layered glass structures were impacted at impact velocities of 200 m/s, 300 m/s, and 400 m/s. In the system with a sum of total glass thickness of 3 mm, first 2 mm thick top glass and 1 mm thick bottom glass placed, then 1 mm thick top glass and 2 mm thick bottom glass placed. In the system with a sum glass thickness of 4 mm, first 3 mm thick top glass and 1 mm thick bottom glass placed, then 1 mm thick top glass and 3 mm thick bottom glass placed. In the system with a sum glass thickness of 5 mm, first 4 mm thick upper glass and 1 mm thick lower glass placed, then 1 mm thick upper glass and 4 mm thick lower glass placed. The representation of these systems is given in Figure 3.22.

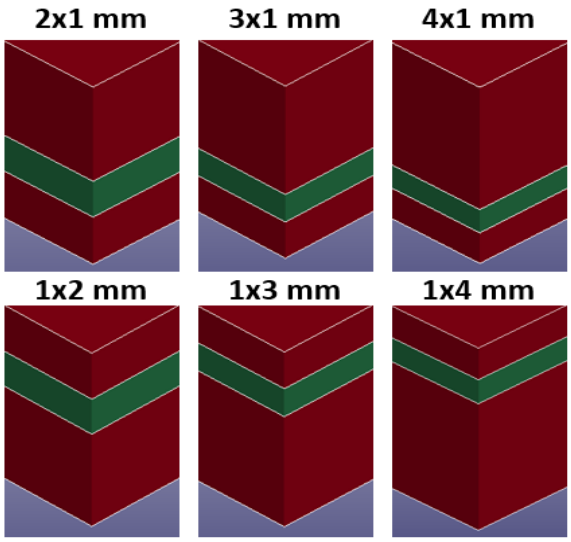

Figure 3.22 Thickness values of the constituents in the layered glass system

Next, 2-glass layer systems with a total glass thickness of 3 mm, 4 mm, and 5 mm were tried with various glass thicknesses and the same 0.76 mm PVB layer thick, with impact velocities of 200 m/s and 400 m/s. The glass thickness combinations of the system, which has a total glass thickness of 3 mm, having the dimensions of 2x1 mm, 1.75x1.25 mm, and 1.25x1.75 mm. The glass thickness combinations of the system with total glass thickness of 4 mm, having the dimensions of 3x1 mm, 2.5x1.5 mm, and 1.5x2.5 mm. The glass thickness combinations of the system with a total glass thickness of 5 mm, having the dimensions of 4x1 mm, 3.5x1.5 mm, 2x3 mm, and 1.5x3.5 mm. The representation of these systems is in Figure 3.23.

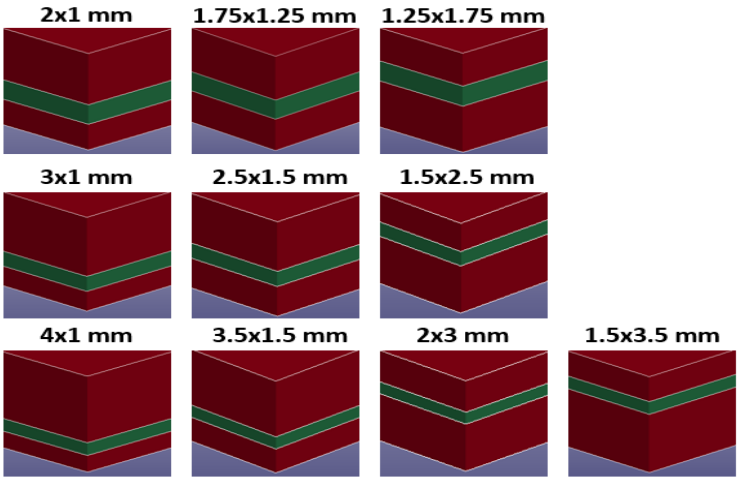

Figure 3.23 The configurations of the layered glass system

The Contact Entity card was defined to support the plate from the bottom. In figure 3.24, a torus was placed under the layered glass structure. Eroding single surface contact type was defined for the layered glass structure and the impactor. Automatic surface to surface tiebreak contact type was used between the glass and PVB parts. The layers were modeled with different density areas. 8-point hexahedron was used with the solid element formulation for the glass and PVB parts. The analysis results are given in detail in Chapter 4.

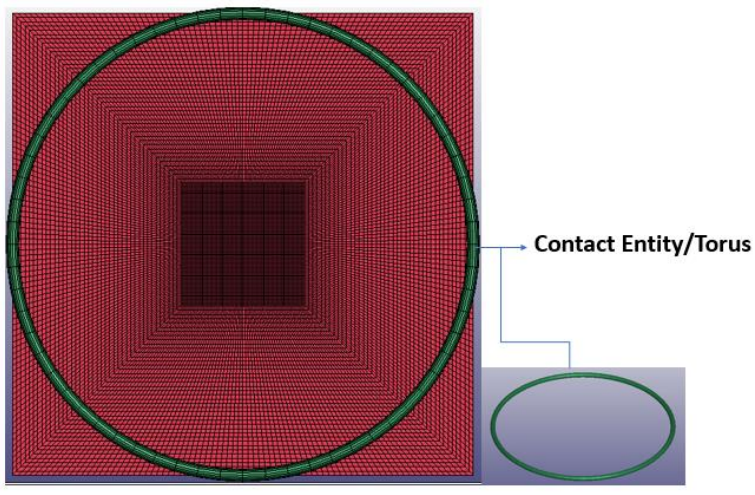

Figure 3.24 Torus shaped bottom support

CHAPTER 4

NUMERICAL RESULTS

In this section, the dynamic compression characteristics of the layered glass are given. In SHPB models, the effect of different types and thicknesses of the interlayer material on stress wave propagation was investigated. In the projectile impact models, the influence of the arrangement of the glass layers with different thicknesses were studied. Finally, the effect of the number of layers are given.

4.1. SHPB Model Results

SHPB is used a controllable wave generation tool, thus it was possible to compare the effect of the parameters studied.

4.1.1. SHPB Model Results of 2-Layer Glass

Cylindrical glass samples with 2 mm thickness and 6 mm diameter were loaded to different incident pulse intensities with peak stress values of 58.50 MPa and 284 MPa. For the low peak incident pulse specimen was deformed elastically. For the high peak incident pulse specimen was deformed catastrophically failed, sudden increase in the reflected pulse indicates the loss of support at the bar ends. As can be seen in Figure 4.1, in the model with a high incident pulse, in a short time, two peaks were formed in the reflected bar in the glass sample.

4.1.2. SHPB Model Results of PVB Layered Glass

The layered glass structure with 0.38 mm, 0.56 mm, 0.76 mm, 1.14 mm, 1.52 mm, and 2.28 mm thick PVB were subjected to dynamic compression loading with two different incident pulses. The dimensions of the layered glass specimens are given in Figure 4.2. The bar responses, and stress-distance-time plot of the layered glass with a PVB interlayer thickness of 0.38 mm are shown in Figure 4.3.

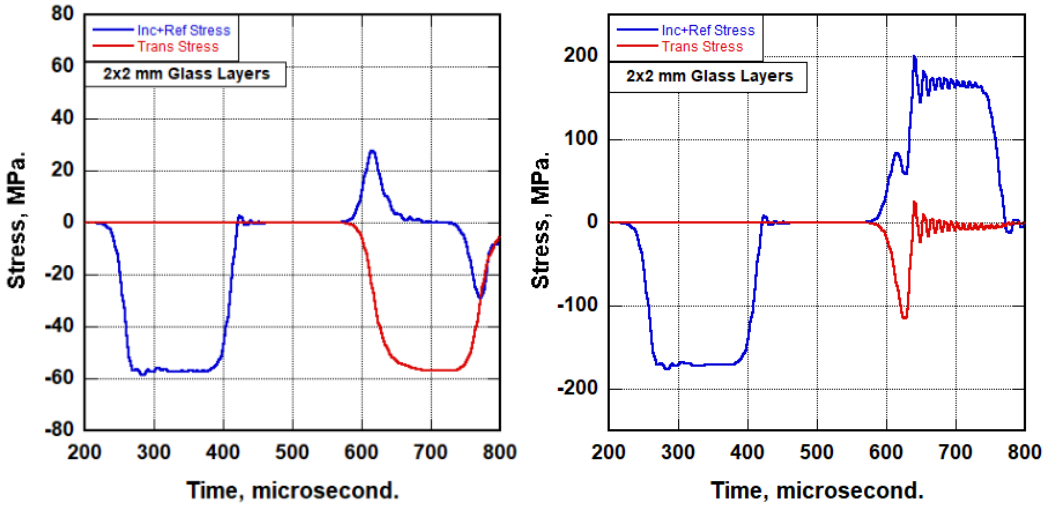

(a) (b)

Figure 4.1 Bar responses of 2-layer glass (a) Incident stress: 58.50 Mpa and (b) Incident Stress: 284 Mpa

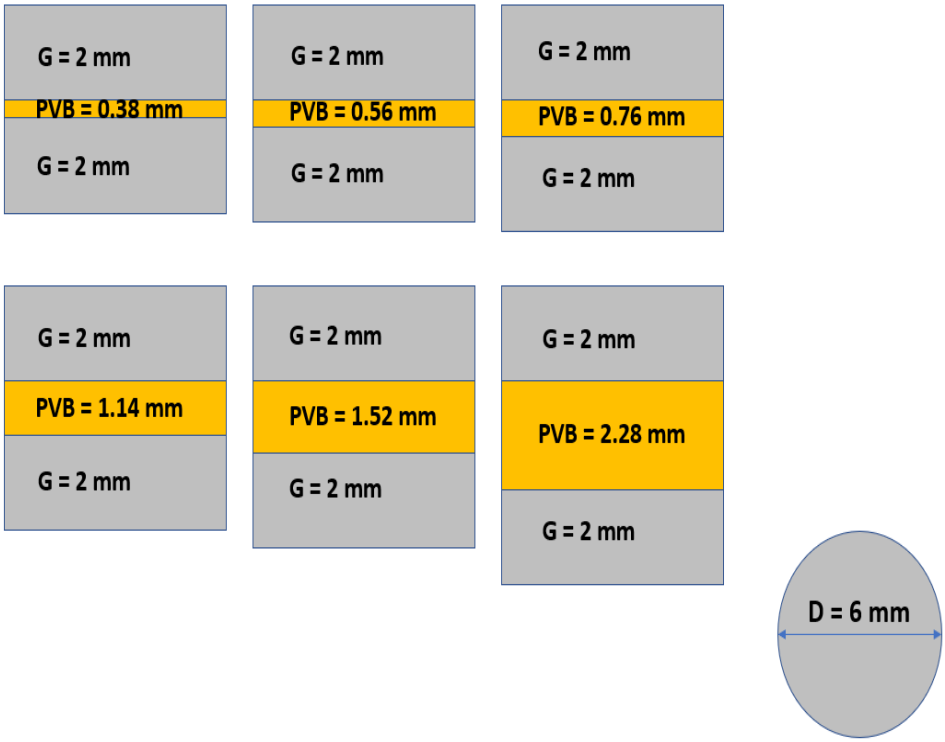

Figure 4.2 Dimension with PVB interlayer of layered glass specimen

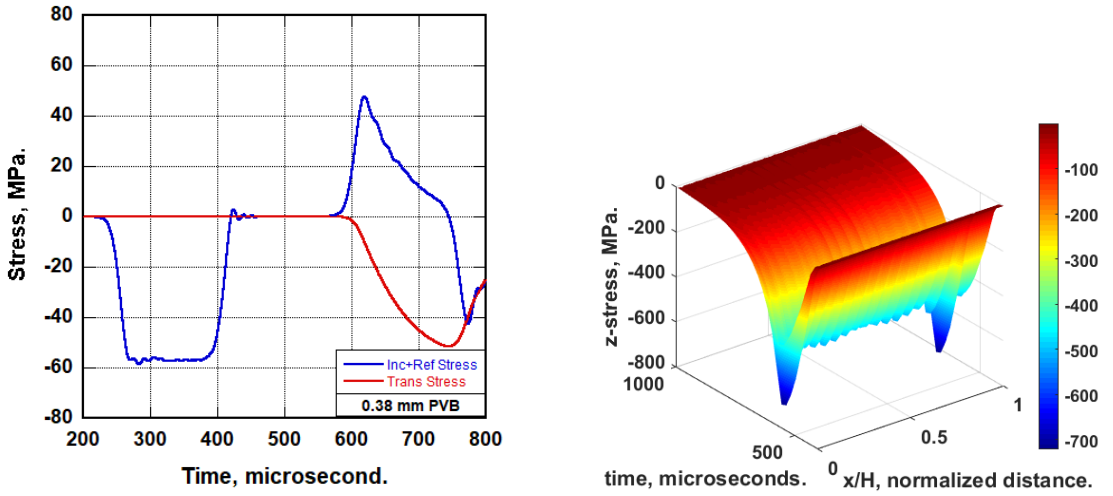

(a)

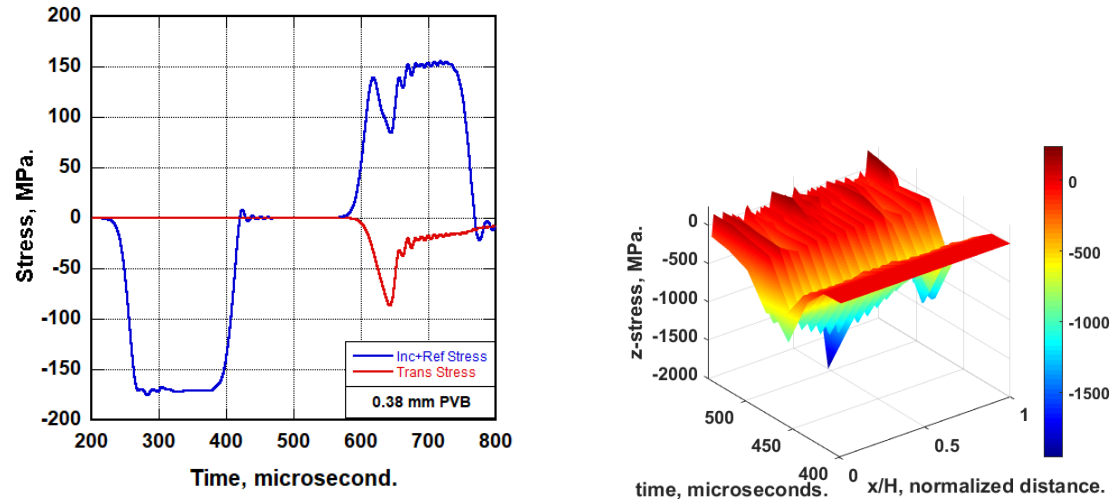

(b)

Figure 4.3 Bar response and stress-distance-time plot of layered glass with 0.38 mm thick PVB (a) Incident stress: 58.50 Mpa and (b) Incident stress: 284 Mpa

The layered glass specimens with 0.38 mm thickness of PVB interlayer were exposed to different incident pulses. For the lower incident pulse, specimen deformed elastically. For the higher incident pulse, specimen was failed. It can be seen that the ends of the specimen experiences higher amounts of stress results a non-uniform stress distribution in the glass layers for the low incident pulse. While, for the high incident pulse, specimen failed and PVB kept the pieces to cause a relatively lower stress distribution. As can be seen in Figure 4.3, in the model with a high incident pulse, in a short time, two peaks were formed in the reflected bar in the glass sample.

The bar responses and stress-distance-time plot of the layered glass with a PVB interlayer thickness of 0.56 mm are represented in Figure 4.4. Similar findings are observed as for the case of 0.38 mm.

The bar responses and stress-distance-time plot of the layered glass with a PVB interlayer thicknesses of 0.76 mm, 1.14 mm, 1.56 mm, and 2.28 mm are represented in Figure 4.5 to 4.8, respectively.

The transmitted and reflected pulses of PVB layered glass are given in Figure 4.9. As can be seen from Figure 4.9 for the low incident pulse, as the thickness of the PVB increased the transmitted pulse was decreased resulting a reduced stress obtained in the glass layers. Increasing the PVB interlayer was found to be effective in stress reduction. For the case of high incident pulse, increasing the interlayer thickness both caused a reduction in the maximum stress and also a significant amount of time delay. Thus, a stress wave mitigational effect was found.

4.1.3. SHPB Model Results of PC Layered Glass

A similar parametric numerical study was performed with varying thickness of PC in order to compare the responses with these of PVB interlayer. Results are given in Figure 4.11. The configurations tried are given in Figure 4.10. This study was done by using low incident pulse.

As can be seen from the Figure 4.12, PC is very effective in stress reductive and for the case investigated the thickness of 0.56 mm and above is good enough for this purpose. In figure 4.13, for the cases studied PC presented more reduction in the stress values obtained in the specimen than those of PVB interlayer used.

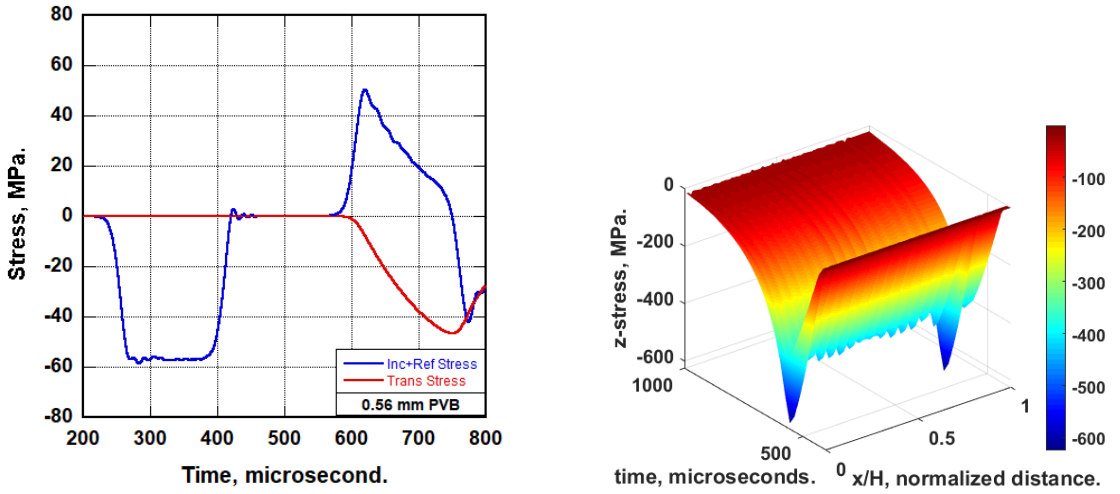

(a)

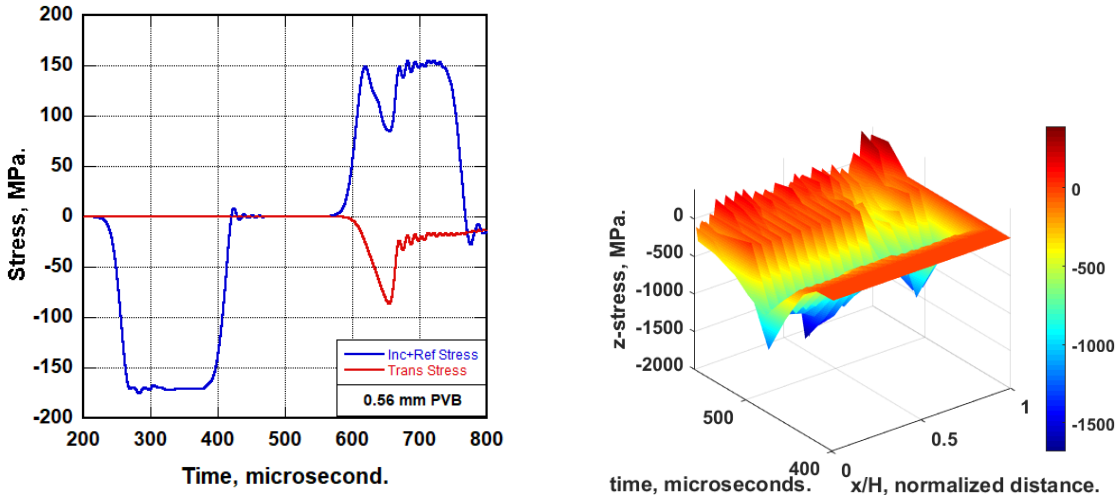

(b)

Figure 4.4 Bar response and stress-distance-time plot of layered glass with 0.56 mm thick PVB (a) Incident stress: 58.50 Mpa and (b) Incident stress: 284 Mpa

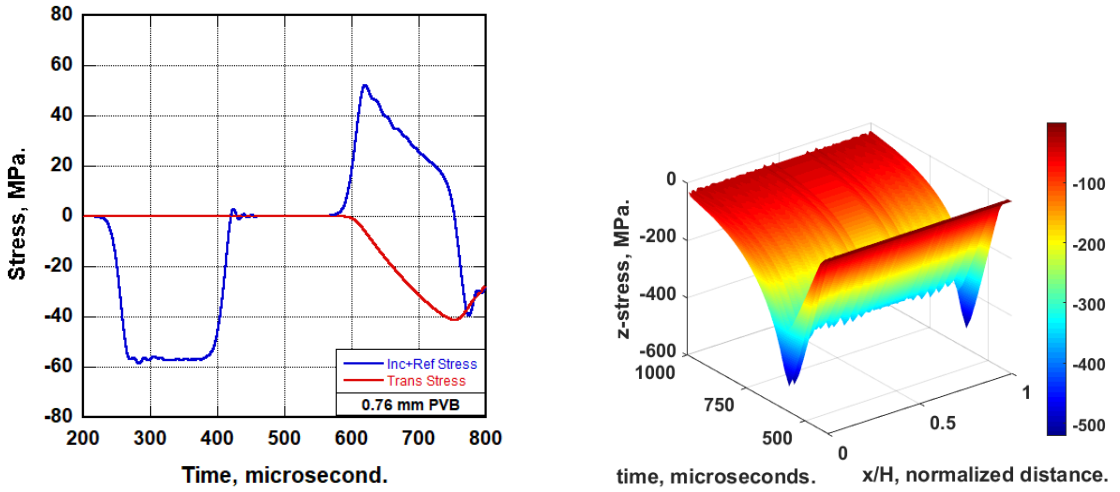

(a)

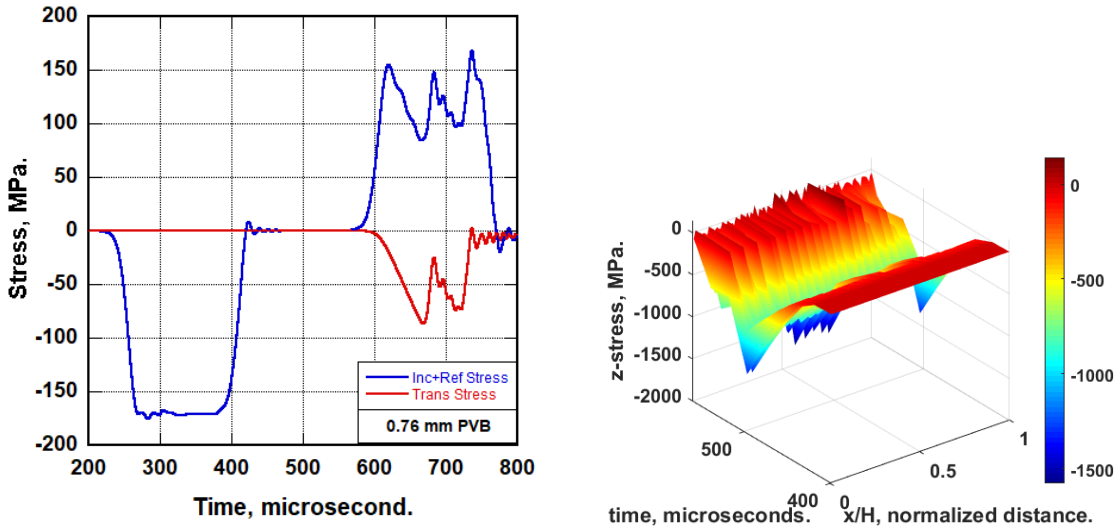

(b)

Figure 4.5 Bar response and stress-distance-time plot of layered glass with 0.76 mm thick PVB (a) Incident stress: 58.50 Mpa and (b) Incident stress: 284 Mpa

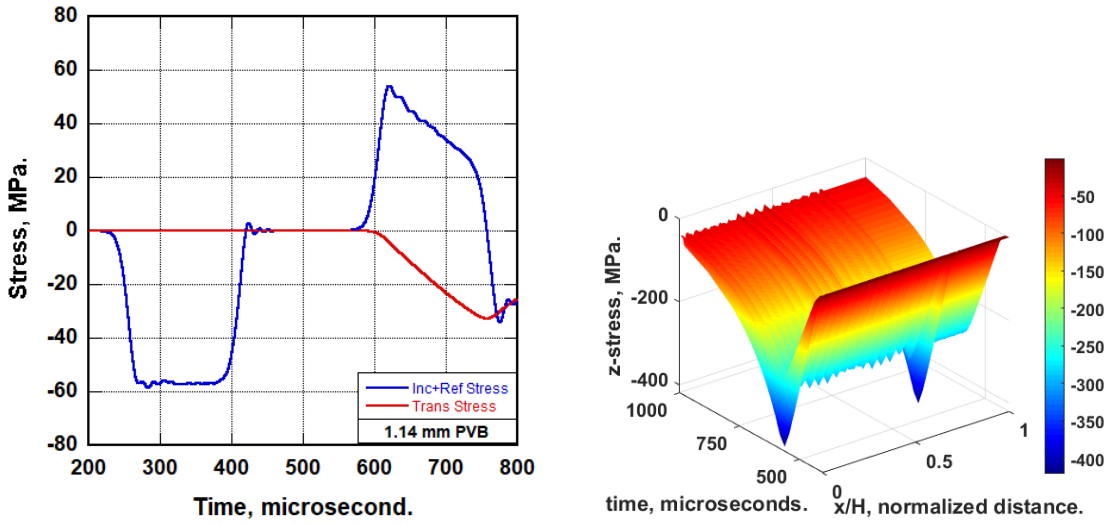

(a)

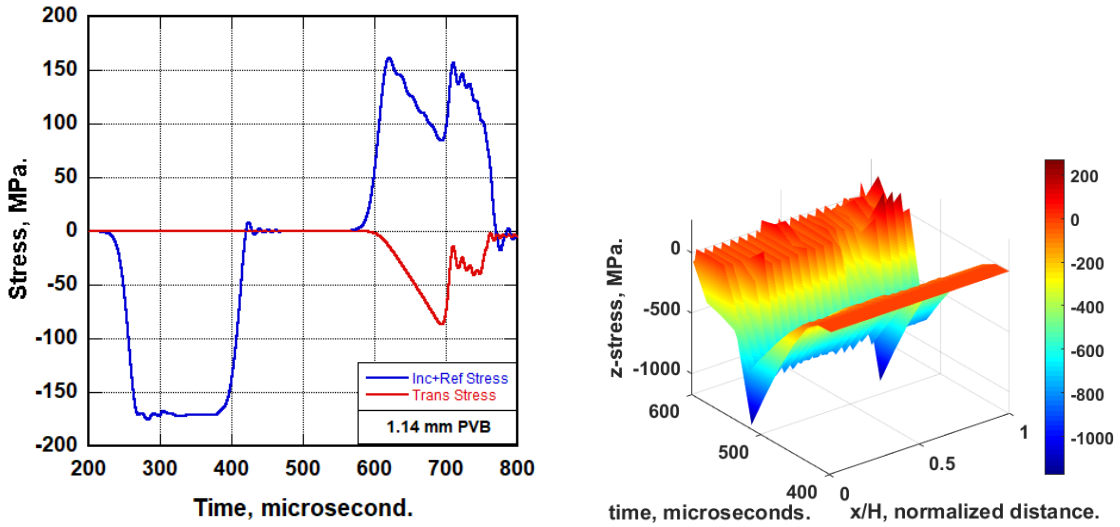

(b)

Figure 4.6 Bar response and stress-distance-time plot of layered glass with 1.14 mm thick PVB (a) Incident stress: 58.50 Mpa and (b) Incident stress: 284 Mpa

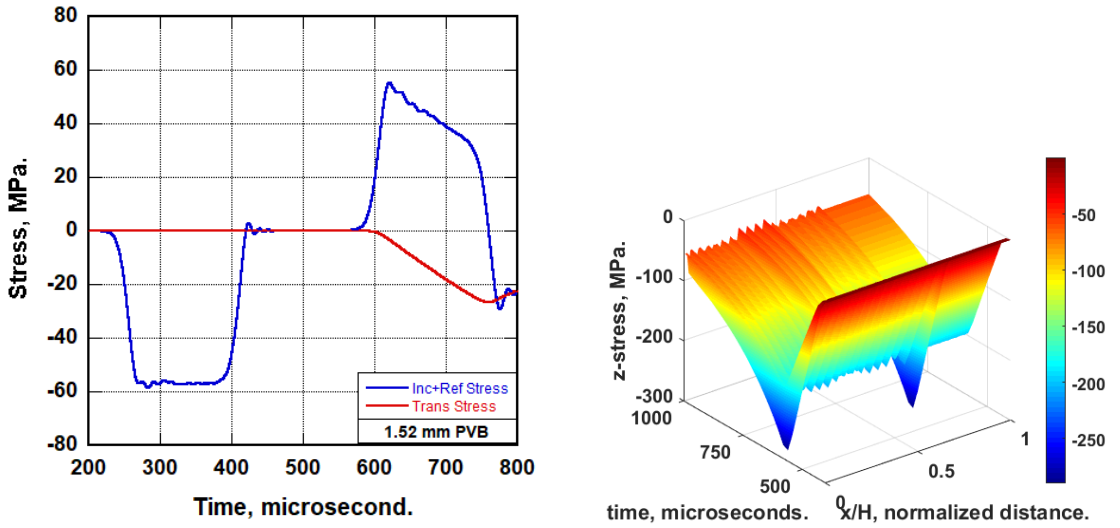

(a)

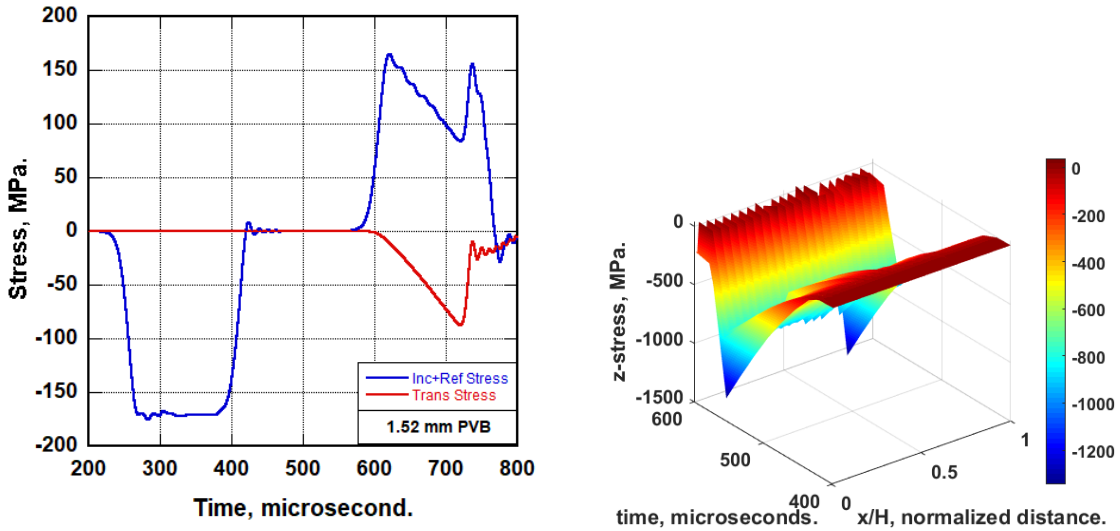

(b)

Figure 4.7 Bar response and stress-distance-time plot of layered glass with 1.52 mm thick PVB (a) Incident stress: 58.50 Mpa and (b) Incident stress: 284 Mpa

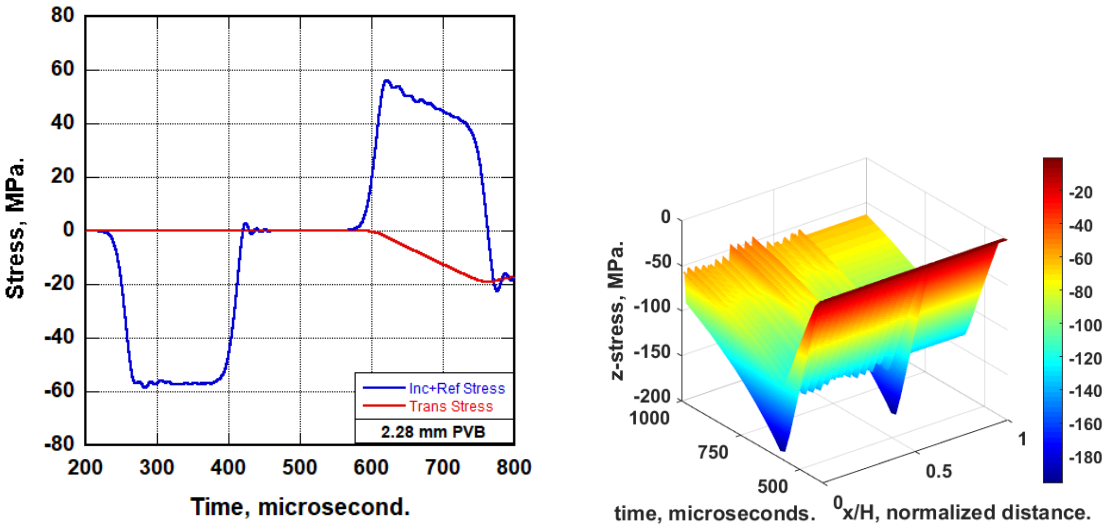

(a)

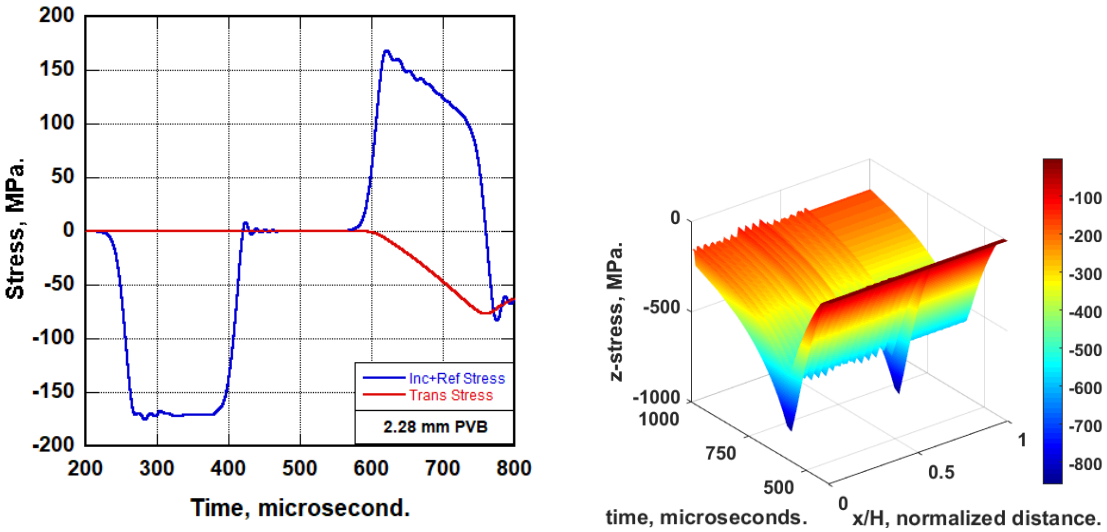

(b)

Figure 4.8 Bar response and and stress-distance-time plot of layered glass with 2.28 mm thick PVB (a) Incident stress: 58.50 Mpa and (b) Incident stress: 284 Mpa

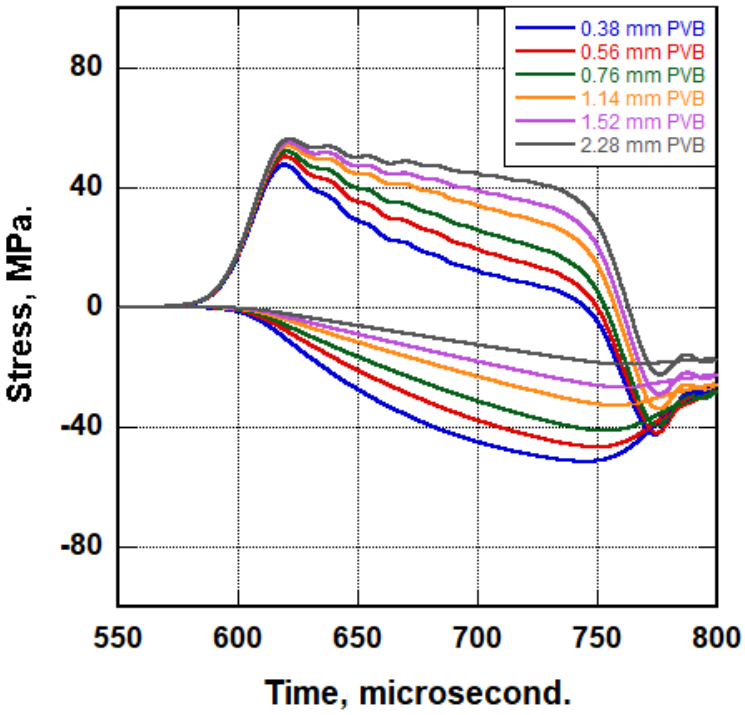

(a)

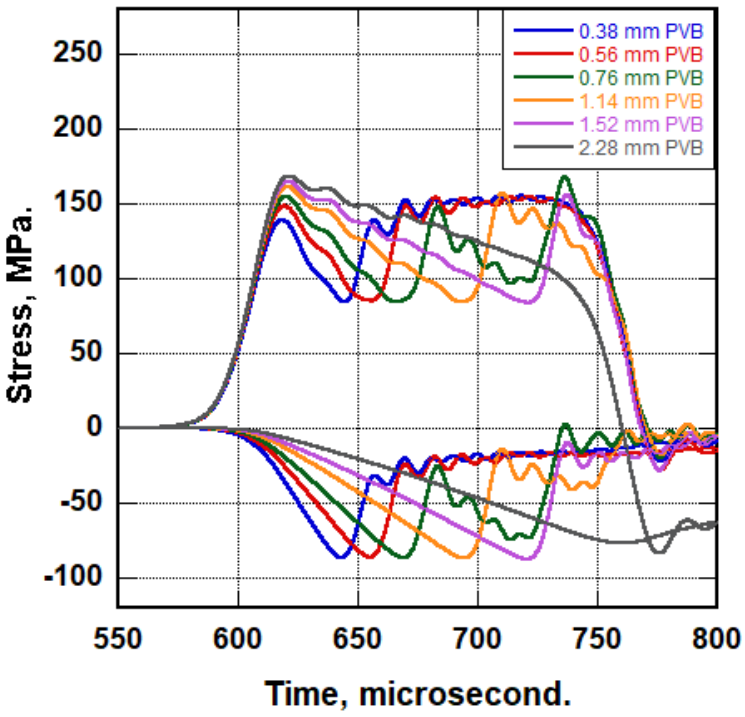

(b)

Figure 4.9 Transmitted and reflected pulses of all cases investigated with PVB

(a) Incident stress: 58.50 Mpa and (b) Incident stress: 284 Mpa

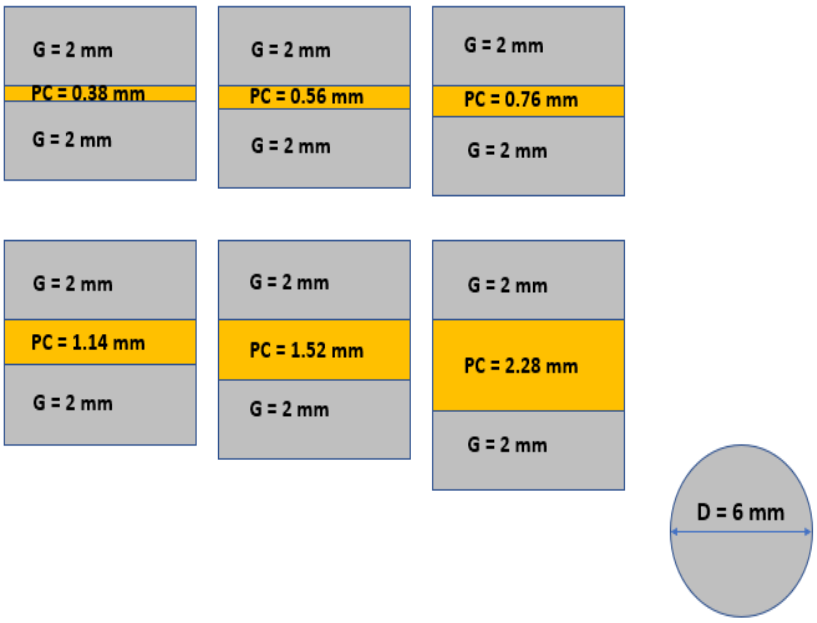

Figure 4.10 Dimension of layered glass specimen with PC interlayer

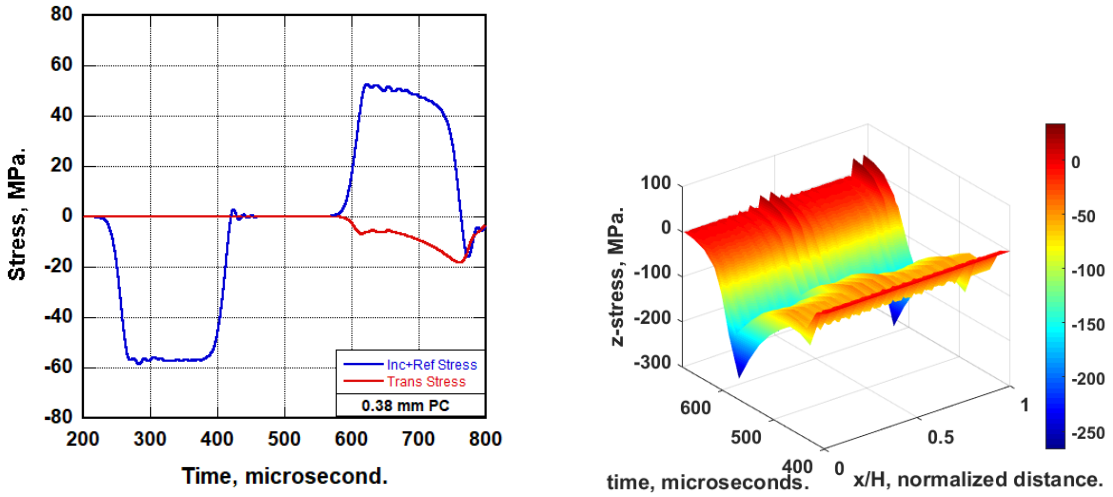

(a)

(cont. on next page)

Figure 4.11 Bar response and and stress-distance-time plot of layered glass with different thick PC; Incident stress: 58.50 Mpa
(a) 0.38 mm thick interlayer, (b) 0.56 mm thick interlayer (c) 0.76 mm thick interlayer, (d) 1.14 mm thick interlayer, (e) 1.52 mm thick interlayer and (f) 2.28 mm thick interlayer

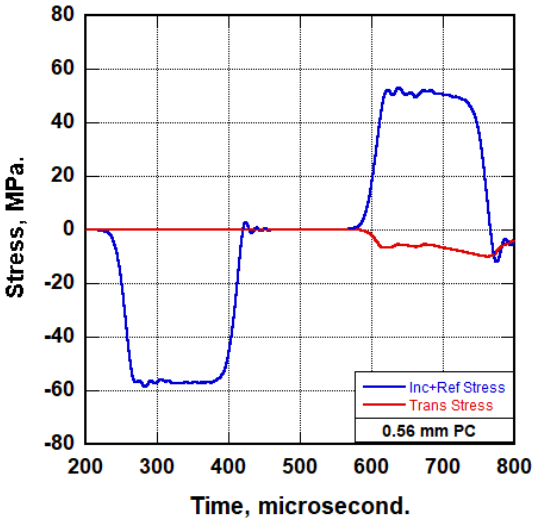

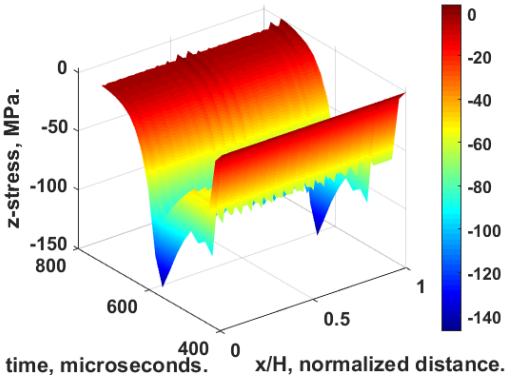

(b)

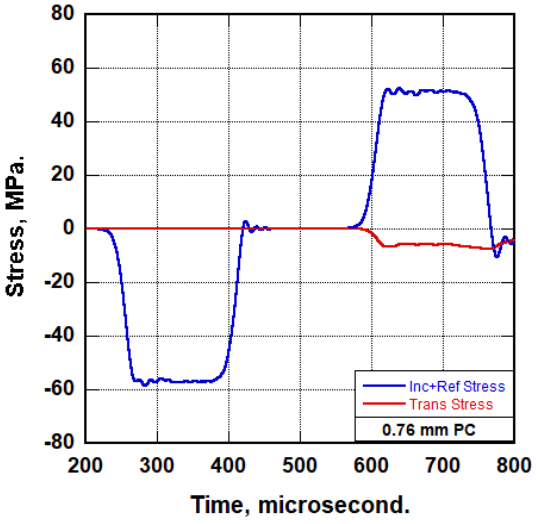

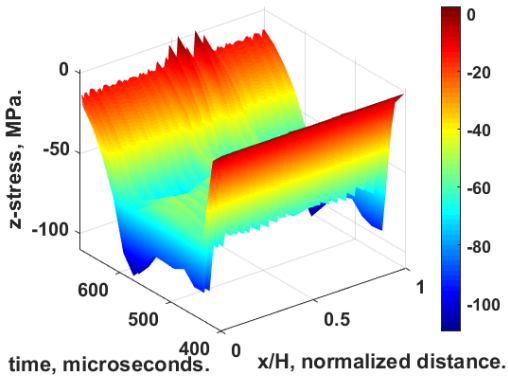

(c)

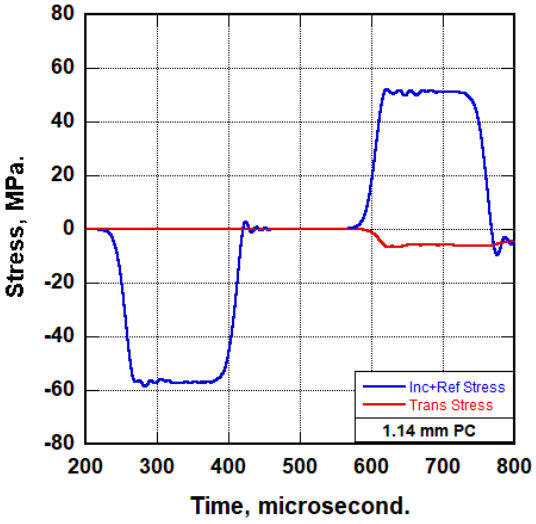

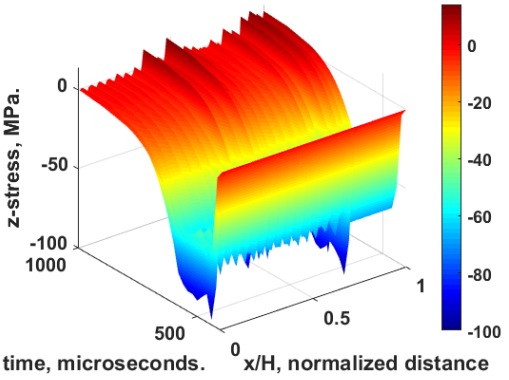

(d)

(cont. on next page)

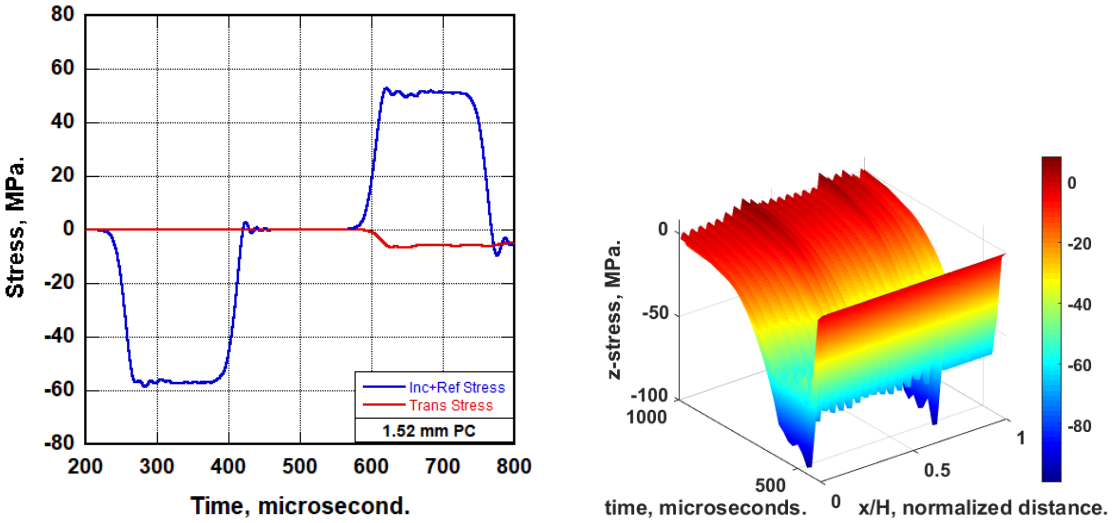

(e)

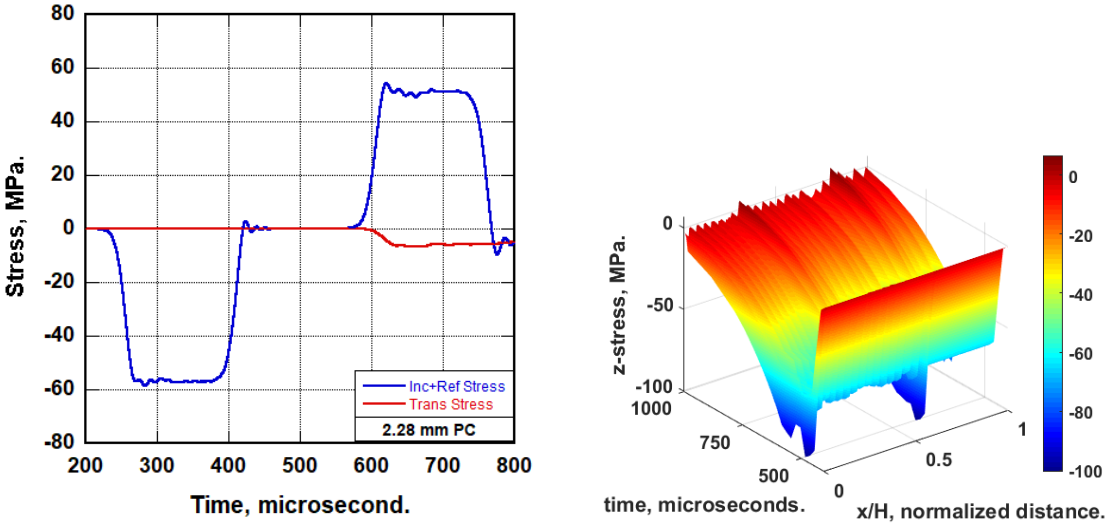

(f)

Figure 4.11 (cont.)

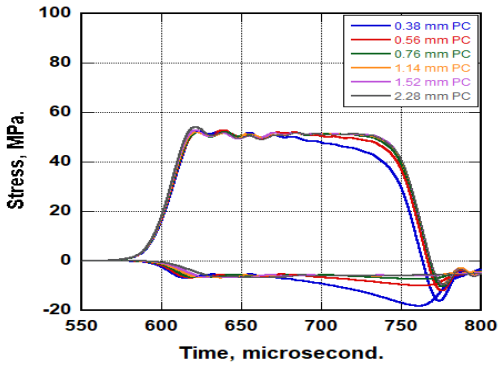

Figure 4.12 Transmitted and reflected pulses of all cases investigated with PC interlayer

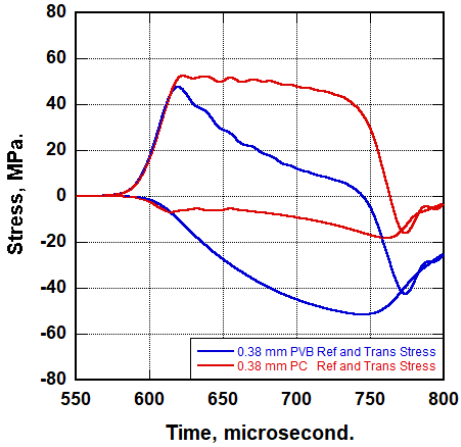

(a)

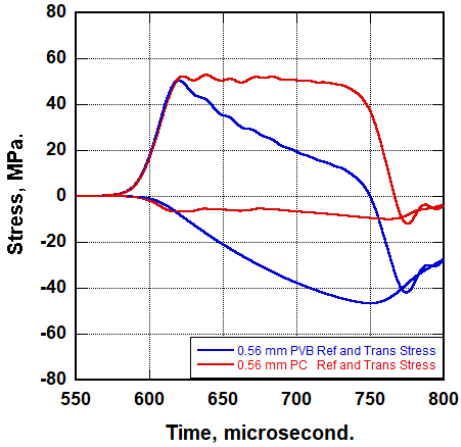

(b)

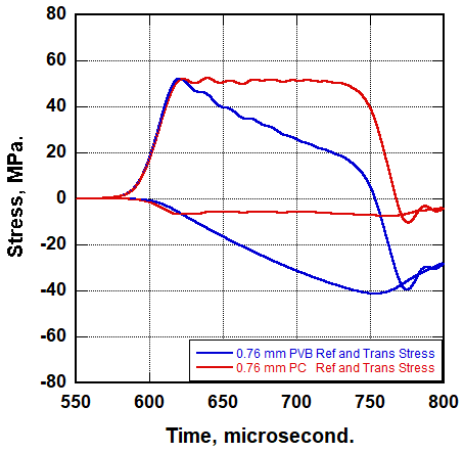

(c)

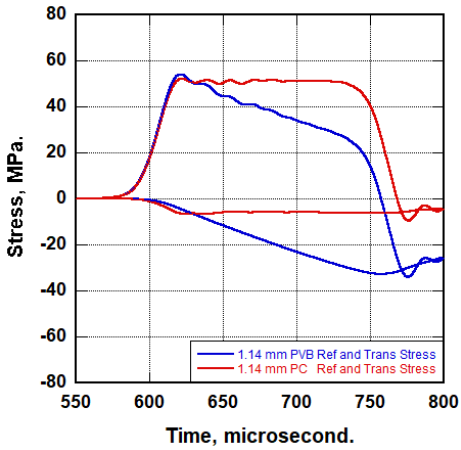

(d)

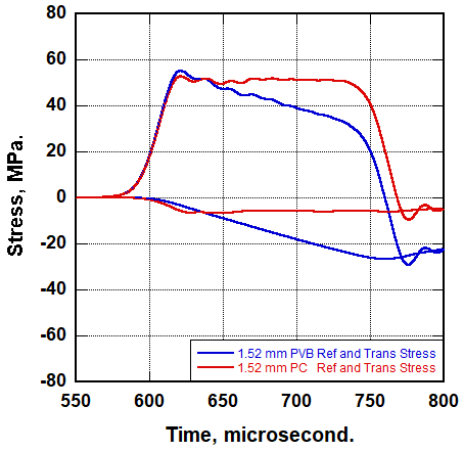

(e)

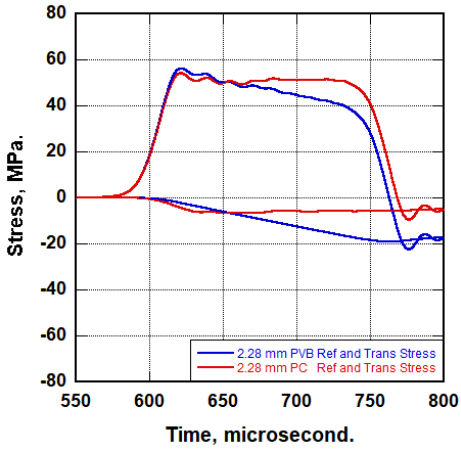

(f)

Figure 4.13 The bar response comparison of different interlayers (a) 0.38 mm thick interlayer, (b) 0.56 mm thick interlayer (c) 0.76 mm thick interlayer, (d) 1.14 mm thick interlayer, (e) 1.52 mm thick interlayer and (f) 2.28 mm thick interlayer

4.2. Projectile Impact Model Results

The results of a projectile impact model for PVB laminated glass with three different configurations are presented.

4.2.1. 2-Layer, 3-Layer, and 4-Layer PVB Layered Glass

For the projectile impact test modeling study, a PVB interlayer was placed between two glass layers (2-Layer), two PVB interlayers between three glass layers (3-Layer), and three PVB interlayers between four glass layers (4-Layer). The thicknesses of the glass and the PVB are 2 mm and 0.76 mm, respectively. The length and width of the plate is 150 mm. Impact velocities between 100 m/s and 500 m/s, were tried, with 8 mm sphere steel projectile. The resultant velocity of the projectile and the amount of eroded energy of the layered glass structure were collected. The dimensions of the layered glass plate are given in Figure 4.14.

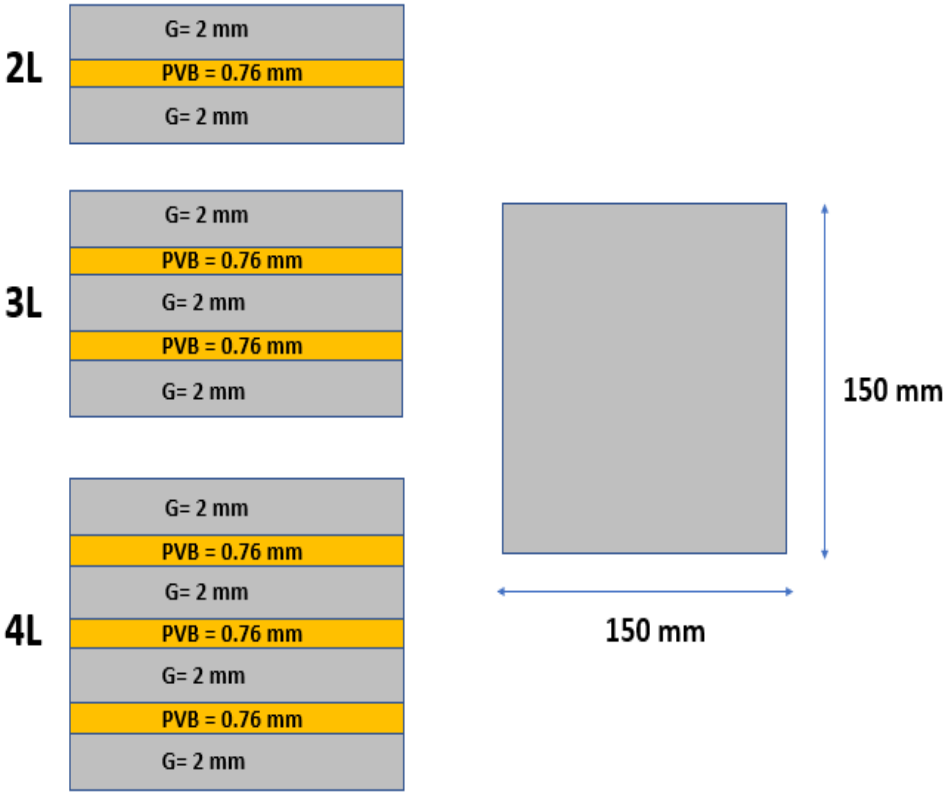

Figure 4.14 Thickness and length measurements of layered glass

4.2.1.1. Resultant Velocity

The resultant velocity of the projectile is given in Figure 4.15 for different initial velocities.

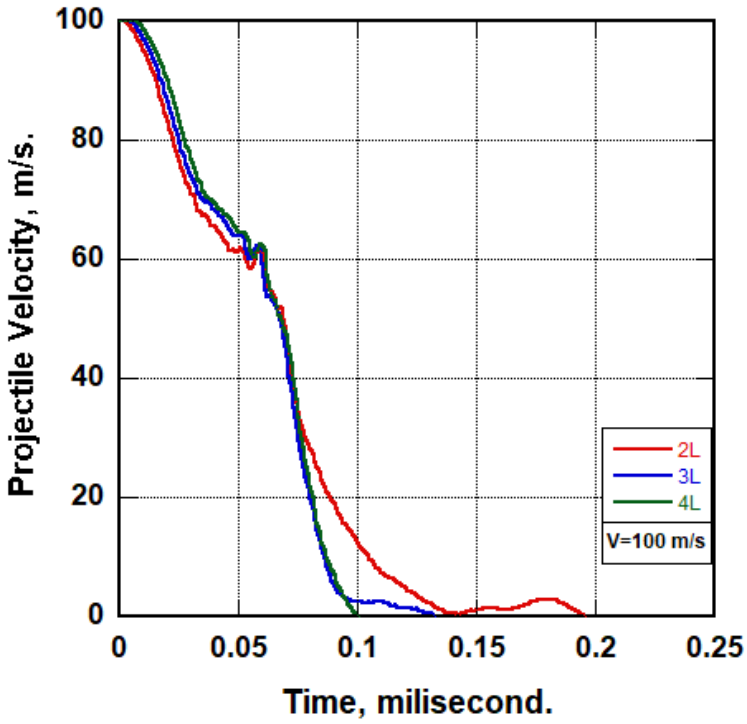

(a)

(cont. on next page)

Figure 4.15 Projectile velocity of 2-Layer, 3-Layer, and 4-Layer layered glass
(a) v=100 m/s, (b) v=150 m/s, (c) v=200 m/s, (d) v=250 m/s, (e) v=300 m/s, (f) v=350 m/s, (g) v=400 m/s, (h) v=450 m/s, and (i) v=500 m/s

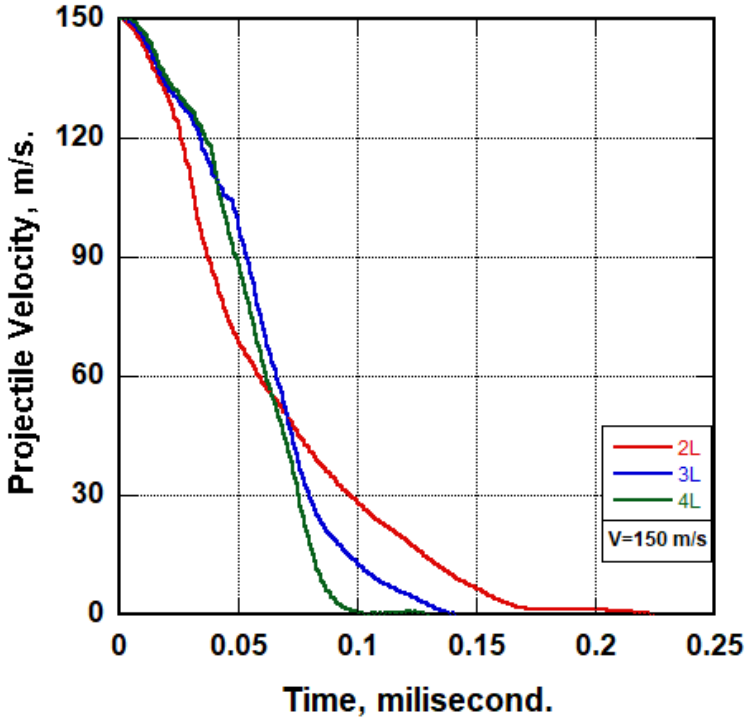

(b)

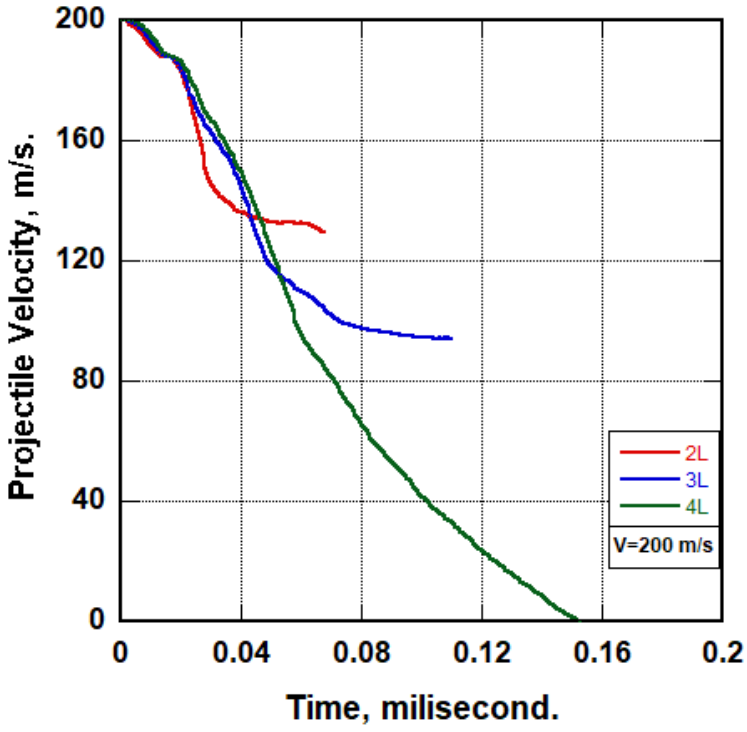

(c)

(cont. on next page)

Figure 4.15 (cont.)

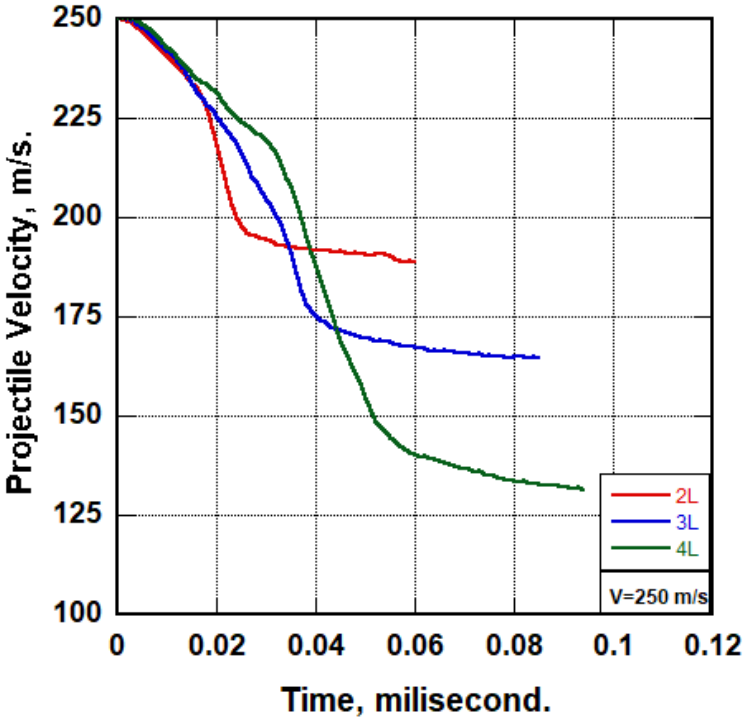

(d)

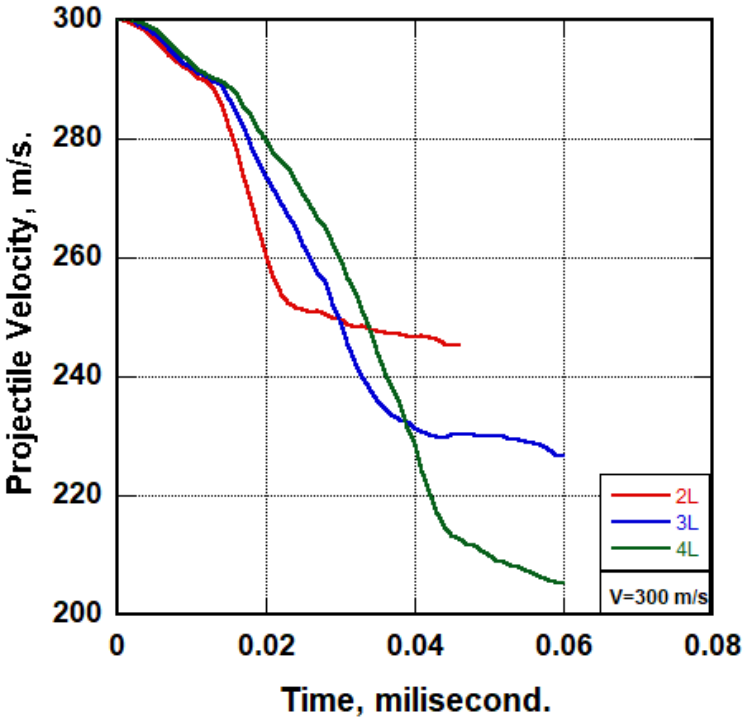

(e)

(cont. on next page)

Figure 4.15 (cont.)

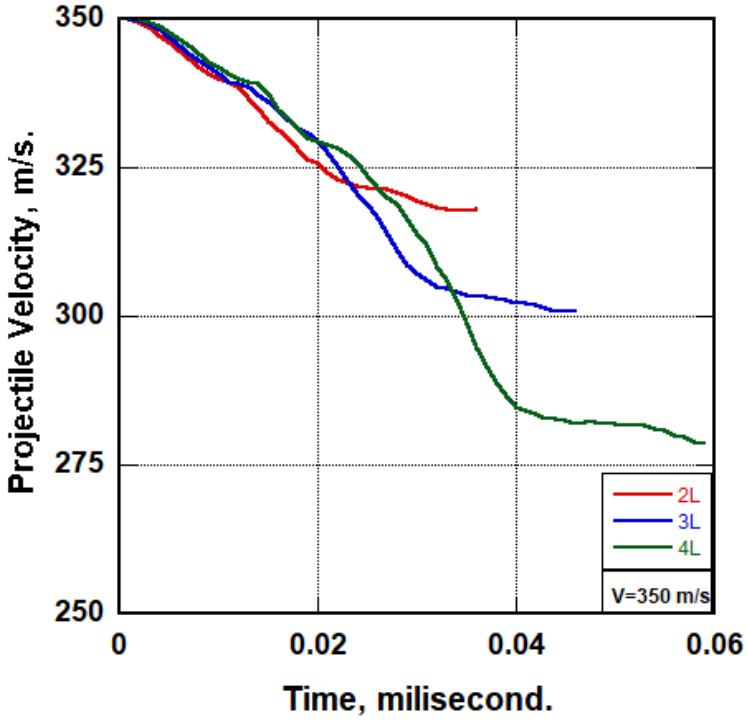

(f)

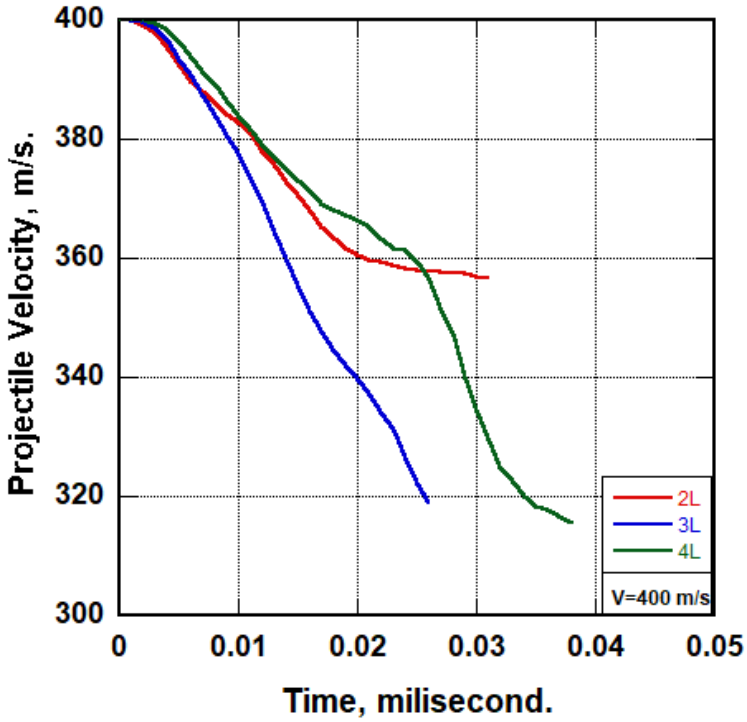

(g)

(cont. on next page)

Figure 4.15 (cont.)

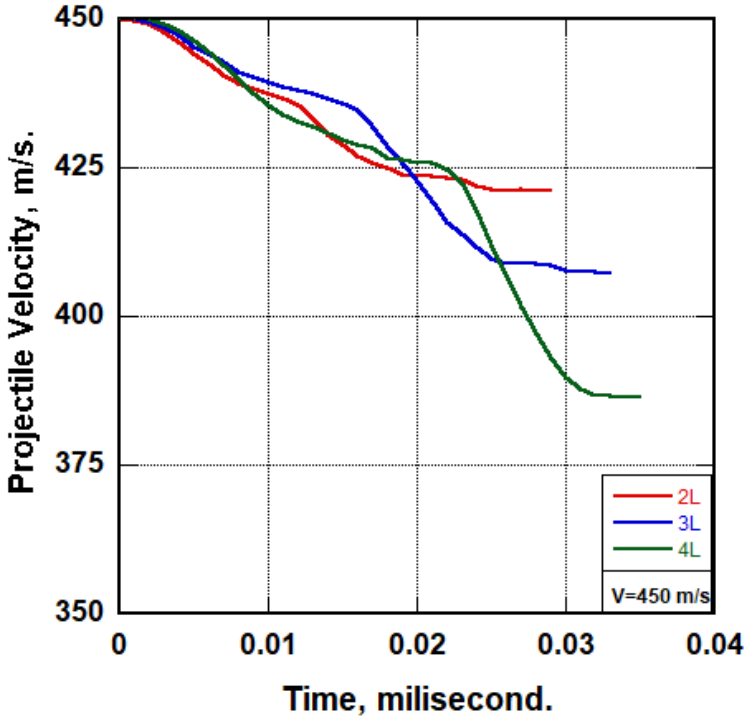

(h)

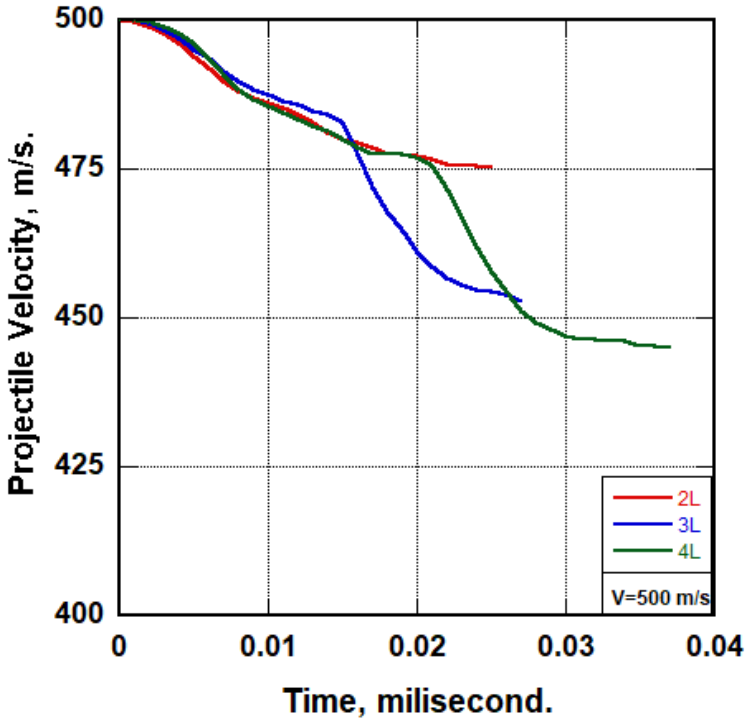

(i)

(cont. on next page)

Figure 4.15 (cont.)

For the 100 and 150 m/s initial velocities, plate was not perforated. While at 200 m/s, 4-Layer plate was able to stop the projectile, though 2-Layer and 3-Layer plates were perforated. After 250 m/s, all the configurations were perforated, and 4-Layer plate was able to decelarate the projectile more as compared to the other two configurations. In Table 4.1 results are summerized.

4.2.1.2. Eroded Energy

The eroded energy histories of different configurations are given in Figure 4.16.

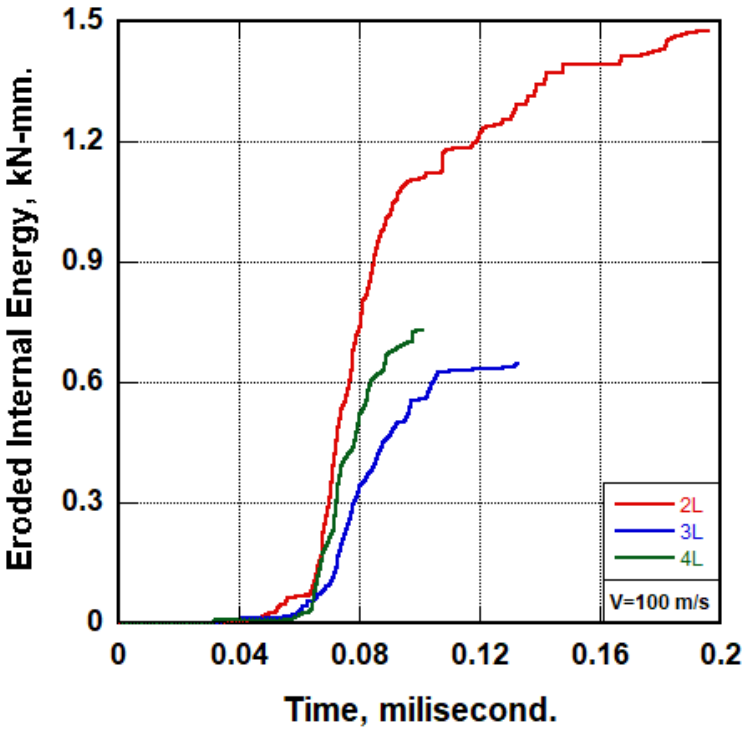

(a)

(cont. on next page)

Figure 4.16 Eroded energy of 2-Layer, 3-Layer, and 4-Layer layered glass systems (a) v=100 m/s, (b) v=150 m/s, (c) v=200 m/s, (d) v=250 m/s, (e) v=300 m/s, (f) v=350 m/s, (g) v=400 m/s, (h) v=450 m/s, and (i) v=500 m/s

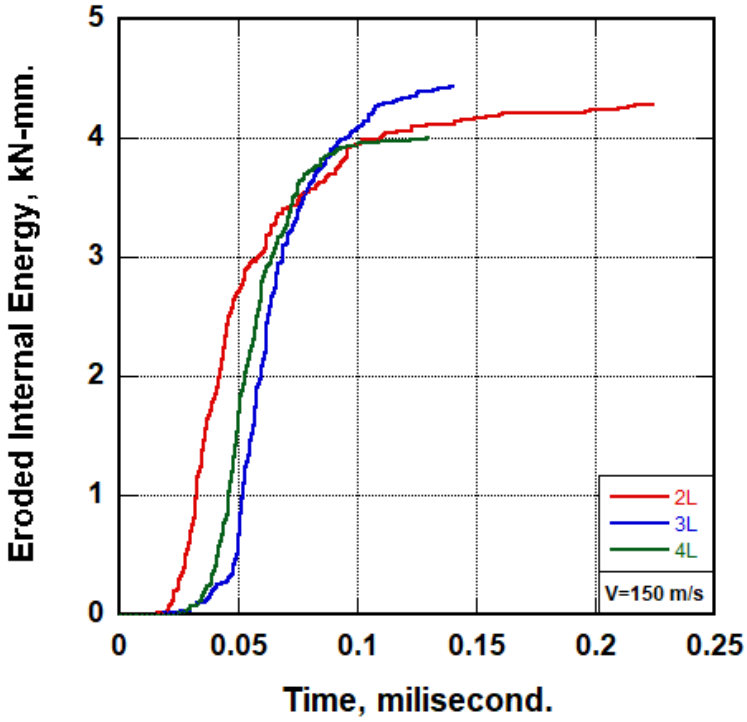

(b)

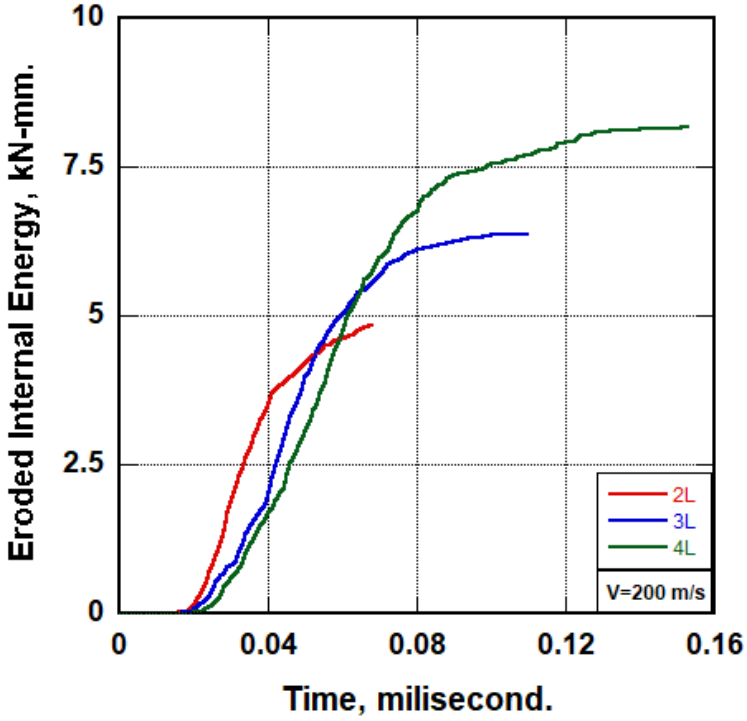

(c)

(cont. on next page)

Figure 4.16 (cont.)

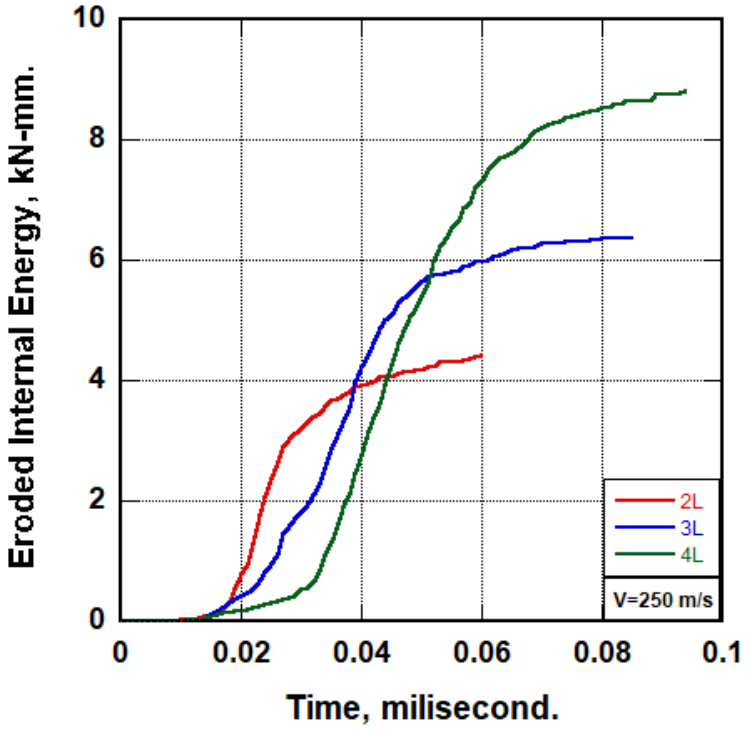

(d)

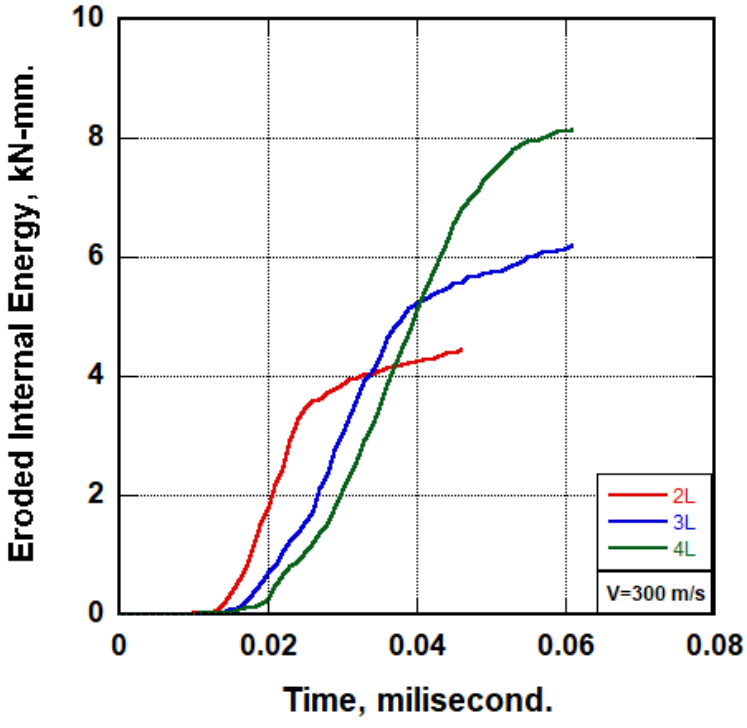

(e)

(cont. on next page)

Figure 4.16 (cont.)

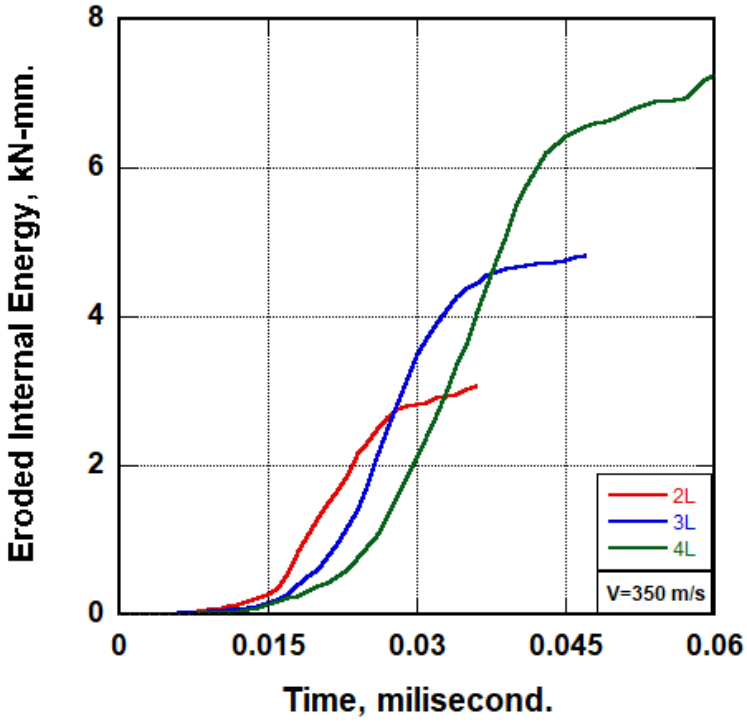

(f)

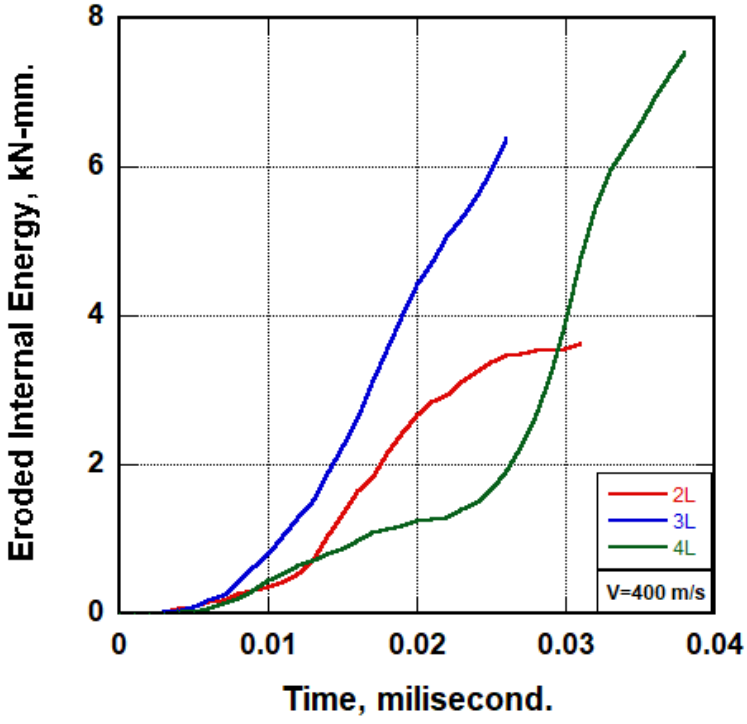

(g)

(cont. on next page)

Figure 4.16 (cont.)

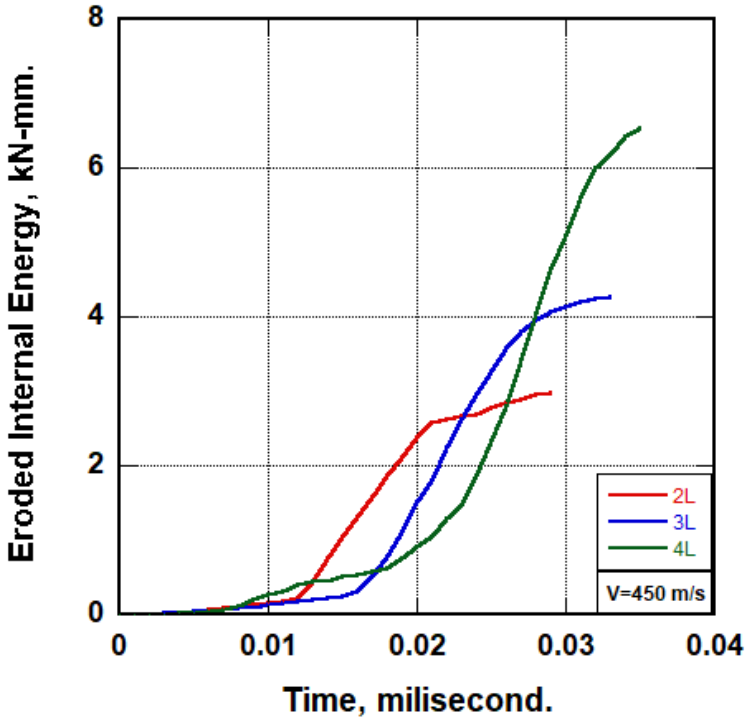

(h)

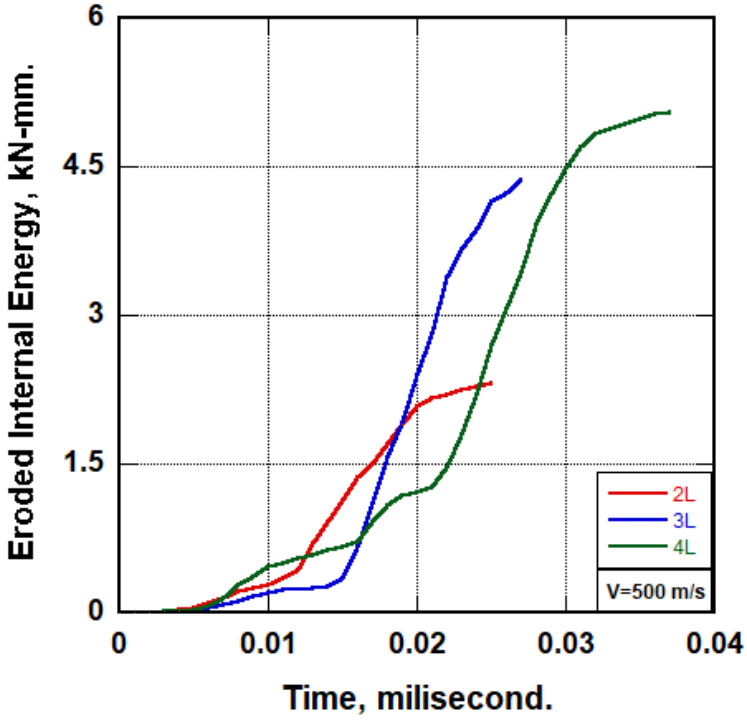

(i)

Figure 4.16 (cont.)

Typical trend observed for any of the cases investigate is that eroded internal energy increases suddenly after 200 m/s and higher values observed at around 300 m/s, therefore decrease of the energy is noted. This may be attributed to the local effects become more pronounced as the impact velocity increases. In Table 4.2 results are summarized.

4.2.1.3. Energy Balance

The total energy of the system is equal to the sum of the kinetic energy, internal energy, spring damper energy, hourglass energy, dumping energy, and sliding energy [34]. Energy balance was cross-checked in the models and consistent values were noted. The total energy results of each model are given in Table 4.3.

4.2.2. Configurations with 1 mm Thick Glass Layer

In this section, different glass layer thickness with 1 mm thick glass were numerically shot with the core projectile at different impact velecoties. The configurations tried are given in Figure 4.17.

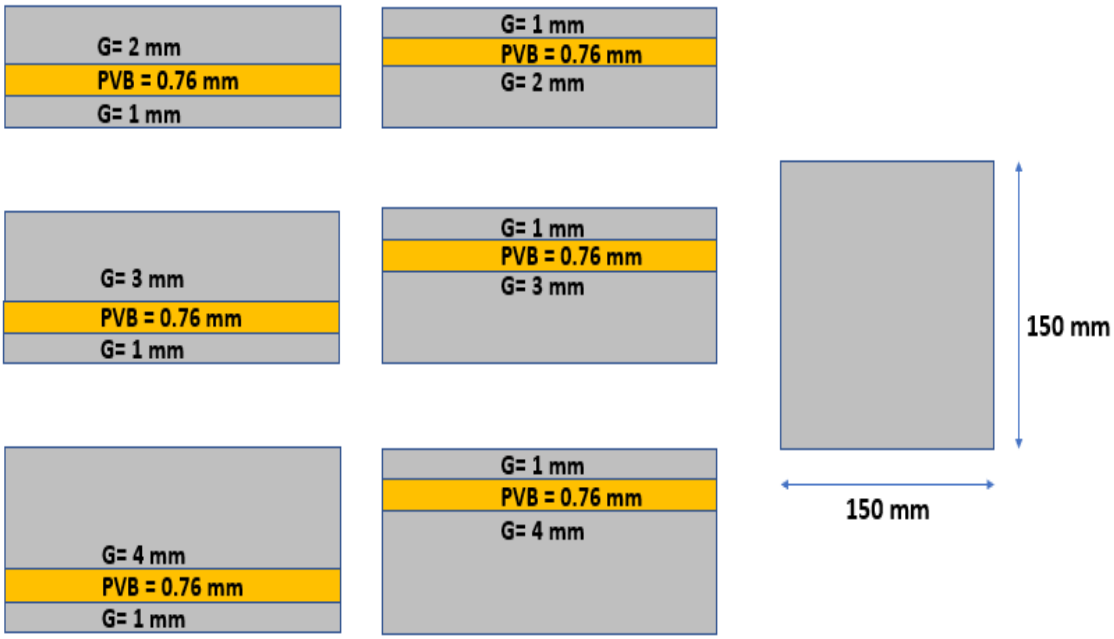

Figure 4.17 Dimensions of the plate

Table 4.1 Resultant velocity results of 2-Layer, 3-Layer, and 4-Layer configurations

Layered Glass System	Initial Velocity (m/s)	Resultant Velocity (m/s)	Deceleration %	Layered Glass System	Initial Velocity (m/s)	Resultant Velocity (m/s)	Deceleration %
2L	100	0	100%	**4L**	300	205.3	31.5%
3L	100	0	100%	**2L**	350	318	9.1%
4L	100	0	100%	**3L**	350	300.7	14.1%
2L	150	0	100%	**4L**	350	278.5	20.41%
3L	150	0	100%	**2L**	400	356.8	10.8%
4L	150	0	100%	**3L**	400	318.8	20.3%
2L	200	129	35.5%	**4L**	400	315.6	21.1%
3L	200	94	53%	**2L**	450	421	6.4%
4L	200	0	100%	**3L**	450	407.3	9.5%
2L	250	188.8	24.5%	**4L**	450	386.3	14.1%
3L	250	164.5	34.2%	**2L**	500	475.2	5.9%
4L	250	131.4	43.4%	**3L**	500	452.7	9.4%
2L	300	245	18.3%	**4L**	500	445	11%
3L	300	226.5	24.5%				

Table 4.2 Eroded energy results of 2-Layer, 3-Layer, and 4-Layer configurations

Layered Glass System	Initial Velocity (m/s)	Eroded Internal Energy (kN-mm)	Layered Glass System	Initial Velocity (m/s)	Eroded Internal Energy (kN-mm)
2-Layer	100	1.48	**4-Layer**	300	8.142
3-Layer	100	0.645	**2-Layer**	350	3.062
4-Layer	100	0.737	**3-Layer**	350	4.83
2-Layer	150	4.3	**4-Layer**	350	7.255
3-Layer	150	4.432	**2-Layer**	400	3.621
4-Layer	150	3.994	**3-Layer**	400	6.371
2-Layer	200	4.82	**4-Layer**	400	7.525
3-Layer	200	6.365	**2-Layer**	450	2.988
4-Layer	200	8.17	**3-Layer**	450	4.266
2-Layer	250	4.417	**4-Layer**	450	6.541
3-Layer	250	6.375	**2-Layer**	500	2.314
4-Layer	250	8.806	**3-Layer**	500	4.372
2-Layer	300	4.45	**4-Layer**	500	5.043
3-Layer	300	6.206			

Table 4.3 Total energy of 2-Layer, 3-Layer, and 4-Layer configurations

Layered Glass System	**Initial Velocity (m/s)**	**Total Energy (kN-mm)**	**Layered Glass System**	**Initial Velocity (m/s)**	**Total Energy (kN-mm)**
2-Layer	100	10.255	**4-Layer**	300	91.149
3-Layer	100	10.307	**2-Layer**	350	126.85
4-Layer	100	10.279	**3-Layer**	350	126.06
2-Layer	150	22.314	**4-Layer**	350	125.98
3-Layer	150	22.319	**2-Layer**	400	165.78
4-Layer	150	22.319	**3-Layer**	400	165.47
2-Layer	200	40.521	**4-Layer**	400	164.68
3-Layer	200	39.781	**2-Layer**	450	210.14
4-Layer	200	38.168	**3-Layer**	450	209.62
2-Layer	250	63.533	**4-Layer**	450	209.37
3-Layer	250	62.904	**2-Layer**	500	259.83
4-Layer	250	61.742	**3-Layer**	500	259.32
2-Layer	300	92.397	**4-Layer**	500	258.95
3-Layer	300	91.872			

4.2.2.1. Resultant Velocity

Initial velocities were 200 and 400 m/s. The results are given in Figure 4.18 and 4.19. At this lower velocity placing a thick bottom glass layer resulted in a higher amount of decrease of projectile velocity. Also, as can be expected by the increase in thickness, reduction of velocity increases. At this higher impact velocity placing thicker glass layers at front resulted in higher amount of reduction in velocity. Results are summerized in Table 4.4.

Table 4.4 Resultant velocity results of configurations with 1 mm thick glass layer

Layered Glass System (mm)	Initial Velocity (m/s)	Resultant Velocity (m/s)	Deceleration %	Layered Glass System (mm)	Initial Velocity (m/s)	Resultant Velocity (m/s)	Deceleration %
2x1	200	154	23%	**2x1**	400	360.3	9.9%
1x2	200	134.4	32.8%	**1x2**	400	373.1	6.7%
3x1	200	151	24%	**3x1**	400	341.4	14.6%
1x3	200	127.3	36.4%	**1x3**	400	362.4	9.4%
4x1	200	152.8	23.6%	**4x1**	400	319.9	20%
1x4	200	120.8	39.6%	**1x4**	400	366.4	8.4%

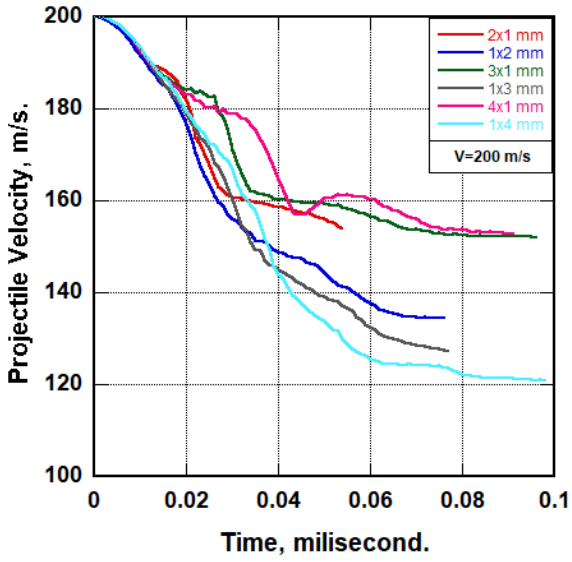

Figure 4.18 Residual velocity of the projectile, initial velocity 200 m/s

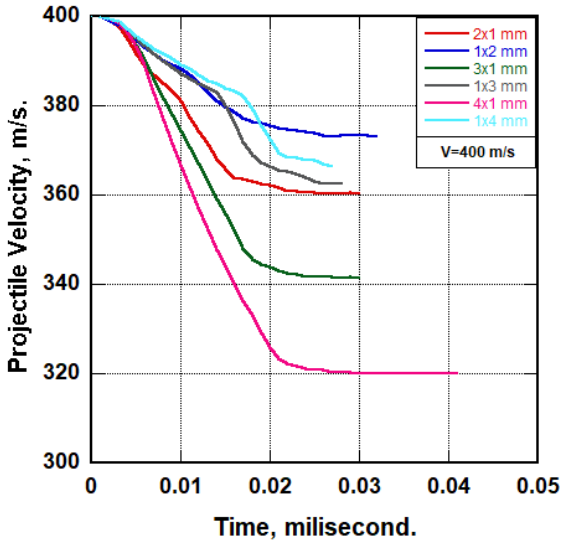

Figure 4.19 Residual velocity of the projectile, initial velocity 400 m/s

4.2.3. Constant Total Thickness Configurations

This time total glass layer thicknesses of 3 mm, 4 mm and 5 mm configurations with different constituent thickness were tried. Dimensions were given in Figure 4.20.

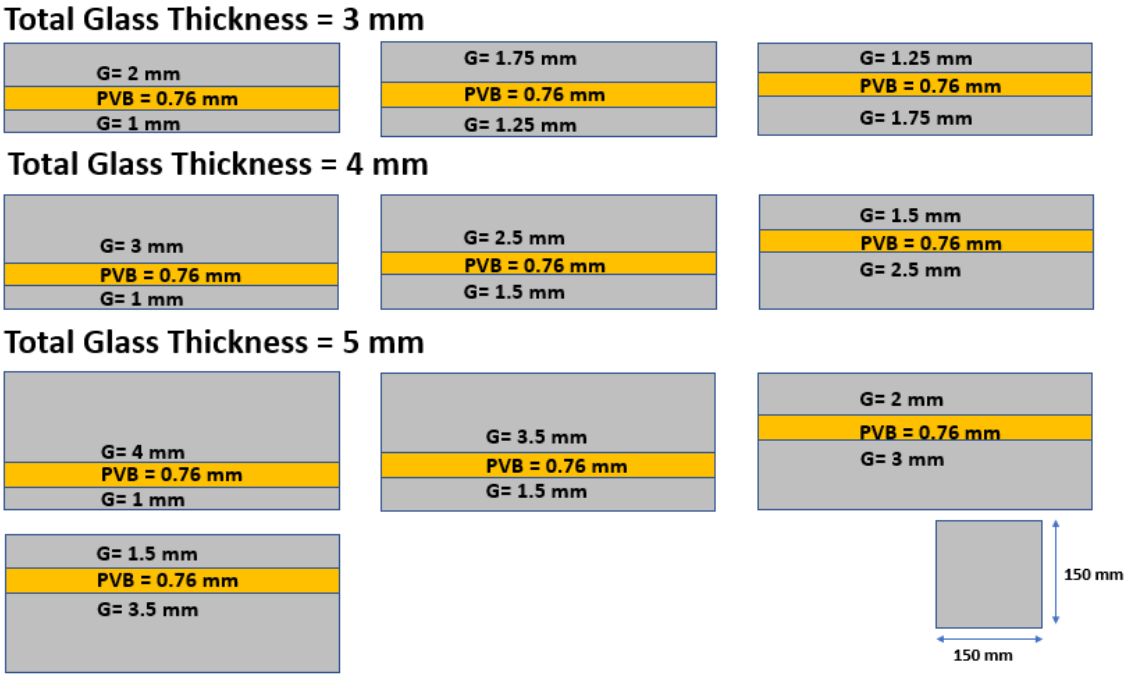

Figure 4.20 Dimensions of the plate

4.2.3.1. Resultant Velocity

Results are summarized in Table 4.5. As can be seen from table, it was possible to increase the amount of reduction by varying the thickness of the layers. At lower velocities placing thicker layers at bottom, while at higher velocities placing thicker layers at top resulted in better responses.

Table 4.5 Resultant velocity results of constant total thickness configurations

Layered Glass System (mm)	**Initial Velocity (m/s)**	**Resultant Velocity (m/s)**	**Deceleration %**	**Layered Glass System (mm)**	**Initial Velocity (m/s)**	**Resultant Velocity (m/s)**	**Deceleration %**
2x1	200	154	33%	**2x1**	400	360.3	9.9%
1.75x1.25	200	149.1	35.4%	**1.75x1.25**	400	353.8	11.5%
1.25x1.75	200	141.7	29.1%	**1.25x1.75**	400	353.4	11.6%
3x1	200	152	24%	**3x1**	400	341.4	14.6%
2.5x1.5	200	134.7	32.6%	**2.5x1.5**	400	343.5	14.1%
1.5x2.5	200	118.6	40.6%	**1.5x2.5**	400	358.6	9.3%
4x1	200	152.8	23.6%	**4x1**	400	319.9	20%
3.5x1.5	200	131.2	34.4%	**3.5x1.5**	400	348.7	12.8%
2x3	200	123.7	38.1%	**2x3**	400	356.1	10.9%
1.5x3.5	200	123.3	38.3%	**1.5x3.5**	400	359.2	10.2%

CHAPTER 5

CONCLUSIONS

In this study, the effect of different interlayer materials, configurations, thickness values on the stress wave propagation in layered glass structures were investigated.

It was found that as the thickness of the interlayer was increased the transmitted stress through the glass structure was decreased for all the interlayer materials in SHPB numerical studies. SHPB numerical simulations also revealed that PC was also effective in reducing the stress values transmitted.

From, the projectile impact simulations, depending on the velocity it was possible to increase the protection efficiency of the structure by placing thicker layers at the bottom for lower velocities, while at the front for the higher impact velocities.

REFERENCES

1. Bulletproof. https://en.wikipedia.org/wiki/Bulletproof_glass.

2. Facades.https://www.guardianglass.com/eu/en/why-glass/build-with-glass/applications-of-glass/glass-for-facades.

3. Aircraft. https://www.swmintl.com/.

4. Automotive.https://www.scienceabc.com/eyeopeners/tempered-laminated-car-windshield-glass-why-break-such-small-pieces.html.

5. Nie, X.; Chen, W. W.; Sun, X.; Templeton, D. W., Dynamic Failure of Borosilicate Glass Under Compression/Shear Loading Experiments. *Journal of the American Ceramic Society* **2007,** *90* (8), 2556-2562.

6. Strassburger, E., High-Speed Transmission Shadowgraphic and Dynamic Photoelasticity Study of Stress Wave and Impact Damage Propagation in Transparent Materials and Laminates Using the Edge-On Impact (EOI) Method. *Army Research Laboratory* **2008**.

7. Grujicic, M.; Pandurangan, B.; Coutris, N.; Cheeseman, B. A.; Fountzoulas, C.; Patel, P.; Templeton, D. W.; Bishnoi, K. D., A simple ballistic material model for soda-lime glass. *International Journal of Impact Engineering* **2009,** *36* (3), 386-401.

8. Peroni, M.; Solomos, G.; Pizzinato, V.; Larcher, M., Experimental Investigation of High Strain-Rate Behaviour of Glass. *Applied Mechanics and Materials* **2011,** *82*, 63-68.

9. Zhang,X; Zou,Y; Hao,H; Li, X; Ma,G; Liu,K., Laboratory Test on Dynamic Material Properties of Annealed Float Glass. *International Journal of Protective Structures* **2012**.

10. Daryadel, S. S., Dynamic Response of Glass under Low-Velocity Impact and High Strain-Rate SHPB Compression Loading. *elsevier* **2015**.

11. Zhang, X.; Hao, H.; Ma, G., Dynamic material model of annealed soda-lime glass. *International Journal of Impact Engineering* **2015,** *77*, 108-119.

12. Sheikh, M. Z.; Wang, Z.; Suo, T.; Li, Y.; Zhou, F.; Ahmed, S.; Dar, U. A.; Wang, Y., Dynamic failure of annealed and chemically strengthened glass under compression loading. *Journal of Non-Crystalline Solids* **2018,** *499*, 189-200.

13. Fu, S.; Wang, Y.; Wang, Y., Tension testing of polycarbonate at high strain rates. *Polymer Testing* **2009,** *28* (7), 724-729.

14. Xu, J.; Li, Y.; Ge, D.; Liu, B.; Zhu, M., Experimental investigation on constitutive behavior of PVB under impact loading. *International Journal of Impact Engineering* **2011,** *38* (2-3), 106-114.

15. Hu, W. J.; Huang, X. C.; Zhang, F. J.; Chen, Y. M., Compression Tests of Polycarbonate under Quasi-Static and Dynamic Loading. *Applied Mechanics and Materials* **2013,** *442*, 125-128.

16. Grant, P. V., The Damage Threshold of Laminated Glass Structures. *Impact Engng* **1998,** *21*, 737-746.

17. Zhao, S.; Dharani, L. R.; Chai, L.; Barbat, S. D., Analysis of damage in laminated automotive glazing subjected to simulated head impact. *Engineering Failure Analysis* **2006,** *13* (4), 582-597.

18. Timmel, M.; Kolling, S.; Osterrieder, P.; Du Bois, P. A., A finite element model for impact simulation with laminated glass. *International Journal of Impact Engineering* **2007,** *34* (8), 1465-1478.

19. Liu, B. H.; Zhu, M. Y.; Sun, Y. T.; Xu, J.; Ge, D. Y.; Li, Y. B., Investigation on Energy Absorption Characteristics of PVB Laminated Windshield Subject to Human Head Impact. *Applied Mechanics and Materials* **2010,** *34-35*, 956-960.

20. Xu, J.; Li, Y.; Liu, B.; Zhu, M.; Ge, D., Experimental study on mechanical behavior of PVB laminated glass under quasi-static and dynamic loadings. *Composites Part B: Engineering* **2011,** *42* (2), 302-308.

21. Thompson, G. M., Detailed Windscreen Model for Pedestrian Head Impact. **2010**.

22. Larcher, M.; Teich, M.; Gebbeken, N.; Solomos, G.; Casadei, F.; Falcon, G. A.; Sarmiento, S. L., Simulation of Laminated Glass Loaded by Air Blast Waves. *Applied Mechanics and Materials* **2011,** *82*, 69-74.

23. Peng, Y.; Deck, C.; Yang, J.; Willinger, R., Modeling and Validation of Windscreen Laminated Glass Behavior during Fracture. In *2012 Third International Conference on Digital Manufacturing & Automation*, 2012; pp 541-544.

24. Liu, B.; Sun, Y.; Li, Y.; Wang, Y.; Ge, D.; Xu, J., Systematic experimental study on mechanical behavior of PVB (polyvinyl butyral) material under various loading conditions. *Polymer Engineering & Science* **2012,** *52* (5), 1137-1147.

25. Zhang, X.; Hao, H.; Ma, G., Laboratory test and numerical simulation of laminated glass window vulnerability to debris impact. *International Journal of Impact Engineering* **2013,** *55*, 49-62.

26. Zhang, X.; Hao, H., Experimental and numerical study of boundary and anchorage effect on laminated glass windows under blast loading. *Engineering Structures* **2015,** *90*, 96-116.

27. Hidallana-Gamage, H. D.; Thambiratnam, D. P.; Perera, N. J., Numerical modelling and analysis of the blast performance of laminated glass panels and the influence of material parameters. *Engineering Failure Analysis* **2014,** *45*, 65-84.

28. Hidallana-Gamage, H. D.; Thambiratnam, D. P.; Perera, N. J., Influence of interlayer properties on the blast performance of laminated glass panels. *Construction and Building Materials* **2015,** *98*, 502-518.

29. Liu, B.; Xu, T.; Xu, X.; Wang, Y.; Sun, Y.; Li, Y., Energy absorption mechanism of polyvinyl butyral laminated windshield subjected to head impact: Experiment and numerical simulations. *International Journal of Impact Engineering* **2016,** *90*, 26-36.

30. Li, K.; Chen, R.; Zhang, H.; Wen, X., The Tensile Properties of PVB at Intermediate Strain Rate Using the In Situ Hopkinson Bar. *Applied Mechanics and Materials* **2015,** *782*, 204-209.

31. Peng, Y.; Ma, W.; Wang, S.; Wang, K.; Gao, G., Investigation of the fracture behaviors of windshield laminated glass used in high-speed trains. *Composite Structures* **2019,** *207*, 29-40.

32. Prasongngen, J., Improvement of windshield laminated glass model for finite element simulation of head-to-windshield impacts. **2019**.

33. Samieian, M. A.; Cormie, D.; Smith, D.; Wholey, W.; Blackman, B. R. K.; Dear, J. P.; Hooper, P. A., On the bonding between glass and PVB in laminated glass. *Engineering Fracture Mechanics* **2019,** *214*, 504-519.

34. LS-DYNA, *LS-DYNA Manual Volume_II_R13*. 2021.

35. Zhao, Y., Yin, H., *Glass Technology*. Chemical Industry Publishing House, 2006.

36. Diehn, B. D. A., *History of Glass*. 1941.

37. Jiu, L., *The history of glass*. 2014.

38. Jun Xu, Y. L., Impact Behavior and Pedestrian Protection of Automotive Laminated Windshield_ Theories, Experiments and Numerical Simulations *Springer Singapore* **2019**.

39. Wang, C. L., S. Tao, Y. Zhang, X., Glass development history and future trends. **Glass (2010)**.

40. Glafo, G., Boken om glas. *Glafo, Växjö, 2nd edition edition,* **2005**.

41. Pilkington The float process,2014.

42. Patterson, M., Structural Glass Facades and Enclosures. *John Wiley & Sons, Inc., Hoboken, New Jersey*, **2011**.

43. Bourhis, E. L., Glass; Mechanics and Technology. *WILEY-VCH Verlag GmbH & Co. KGaA, Weinheim,* **2008**.

44. Fors, C., Mechanical Properties of Interlayers in Laminated Glass Experimental and Numerical Evaluation **2014**.

45. Collins, E. F., Electrically Heated Glass Annealing Lehr. *Journal of the American Ceramic Society* **1921,** *4(5),* 335-349.

46. Meenu Teotia , R. K. S., Polymer Interlayers for Glass Lamination-A Review. *International Journal of Science and Research* **2012**.

47. Haldimann, M. L., Andreas_ Overend, Mauro, Structural Use of Glass. **2008**.

48. Gy, R., Creep and recovery of a thermally tempered glass plate at room temperature. *Proceeding of the Sixth International Conference on Architectural and Automotive Glass, Finland,* **13-16 June,1999.**

49. Istructe, *Structural Use of Glass in Buildings London*. Institution of Structural Engineers: 1999.

50. Per-Olof, C., Bygga med glas. *Ljunbergs Tryckeri AB* **2005**.

51. Martín, M.; Centelles, X.; Solé, A.; Barreneche, C.; Fernández, A. I.; Cabeza, L. F., Polymeric interlayer materials for laminated glass: A review. *Construction and Building Materials* **2020,** *230*.

52. Roff, W. J. S., J.R., *Fibres, Films, Plastics and Rubbers*. A Handbook of Common Polymer: Butterworths, London,, 1971.

53. Elziere, P. Laminated Glass: Dynamic Rupture of Adhesion. Thesis. Université Pierre et Marie Curie, Paris VI,, 2016.

54. Tupý, M.; Meřinská, D.; Svoboda, P.; Zvoníček, J., Influence of water and magnesium ion on the optical properties in various plasticized poly(vinyl butyral) sheets. *Journal of Applied Polymer Science* **2010**.

55. Christensen, R. M., *Theory of viscoelasticity*. Dover Civil and Mechanical Engineering, 1982.

56. Iwasaki, R.; Sato, C.; Latailladeand, J. L.; Viot, P., Experimental study on the interface fracture toughness of PVB (polyvinyl butyral)/glass at high strain rates. *International Journal of Crashworthiness* **2007,** *12* (3), 293-298.

57. Kajon, G. M., L.; and Steindler, R., Monitored ballistic tests on shockproof sandwich glasses. *Exper. Tech* **2001,** (25 (5)), p 27-31.

58. Diewen, S., Discussion on technology of laminated glass. *Glass 42* **2015**.

59. Jun, X. W., Production of printed curvature laminated glass for front windshield of car. *Glass 31, 53–56* **2004**.

60. Liu, Z. P., S., Energy-Saving Glass and Green Glass. *Chemical Industry Publishing House* **2009**.

61. Kott, A. a. V., T. , Safety of laminated glass structures after initial failure. *In Proceedings of the IABSE Symposium Shanghai* **September 22-24. 2004.**

62. Sedlacek, G., Blank, K., Laufs, W. and Güsgen, J. , Glas im Konstruktiven Ingenieurbau. *Ernst & Sohn, Berlin,* **1999**.

63. Gray, G., Classic Split-Hopkinson Pressure Bar Testing. *ASM International* **2000,** *8*, 462–476.

64. Johnson, G. R.; Holmquist, T. J., An improved computational constitutive model for brittle materials. In *AIP Conference Proceedings*, 1994; pp 981-984.

65. Ogden, R. W., Non-Linear Elastic Deformations. *John Wiley % Sons* **1985**.

66. Kolling et al., SAMP-1: A Semi-Analytical Model for the Simulation of Polymers. *Researchgate* **2005**.

67. Holmquist, T. J., Johnson, G.R., Grady, D.E., Lopatin, C.M., Hertel, E.S., Proceedings of fifteenth international symposium on ballistics. **1995**.